Journal of Medicinal Chemistry

ARTICLE

pubs.acs.org/jmc

Discovery and Optimization of a Series of Benzothiazole Phosphoinositide 3-Kinase (PI3K)/Mammalian Target of Rapamycin (mTOR) Dual Inhibitors

Noel D. D'Angelo,[*,†] Tae-Seong Kim,[†] Kristin Andrews,[‡] Shon K. Booker,[†] Sean Caenepeel,[§] Kui Chen,[⊥] Derin D'Amico,[†] Dan Freeman,[§] Jian Jiang,[#] Longbin Liu,[†] John D. McCarter,[⊥] Tisha San Miguel,[⊥] Erin L. Mullady,[¶] Michael Schrag,[#] Raju Subramanian,[#] Jin Tang,[○] Robert C. Wahl,[⊥] Ling Wang,[§] Douglas A. Whittington,[○] Tian Wu,[∥] Ning Xi,[†] Yang Xu,[#] Peter Yakowec,[○] Kevin Yang,[†] Leeanne P. Zalameda,[⊥] Nancy Zhang,[§] Paul Hughes,[§] and Mark H. Norman[†]

Departments of [⊥]High-Throughput Screening/Molecular Pharmacology, [†]Medicinal Chemistry, [‡]Molecular Structure, [§]Oncology Research, [∥]Pharmaceutics, and [#]Pharmacokinetics and Drug Metabolism, Amgen Inc., One Amgen Center Drive, Thousand Oaks, California 91320-1799, United States

Departments of [¶]High-Throughput Screening/Molecular Pharmacology and [○]Molecular Structure, Amgen Inc., 360 Binney Street, Cambridge, Massachusetts 02142, United States

Supporting Information

ABSTRACT: Phosphoinositide 3-kinase α (PI3Kα) is a lipid kinase that plays a key regulatory role in several cellular processes. The mutation or amplification of this kinase in humans has been implicated in the growth of multiple tumor types. Consequently, PI3Kα has become a target of intense research for drug discovery. Our studies began with the identification of benzothiazole compound **1** from a high throughput screen. Extensive SAR studies led to the discovery of sulfonamide **45** as an early lead, based on its in vitro cellular potency. Subsequent modifications of the central pyrimidine ring dramatically improved enzyme and cellular potency and led to the identification of chloropyridine **70**. Further arylsulfonamide SAR studies optimized in vitro clearance and led to the identification of **82** as a potent dual inhibitor of PI3K and mTOR. This molecule exhibited potent enzyme and cell activity, low clearance, and high oral bioavailability. In addition, compound **82** demonstrated tumor growth inhibition in U-87 MG, A549, and HCT116 tumor xenograft models.

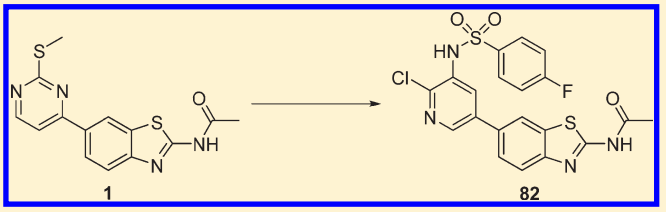

INTRODUCTION

Phosphoinositide 3-kinases (PI3Ks) are a family of lipid kinases that play key regulatory roles in cell proliferation, survival, and cell translation. The PI3K's are divided into three classes based on structural differences and in vitro substrate specificity.[1−3] Class I PI3Ks, which utilize both a catalytic and a regulatory subunit, catalyze the phosphorylation of the 3′-OH position of phosphatidylinositol 4,5-biphosphate (PIP2) to generate phosphatidylinositol 3,4,5-triphosphate (PIP3).[4,5] The phosphatase and tensin homologue gene (PTEN) catalyze the dephosphorylation process, thereby providing a feedback mechanism to regulate the amount of PIP3 that is generated.[6−9] This regulation is important for maintaining normal cell growth because the generation of PIP3 leads to the downstream activation of serine−threonine kinase Akt (AKT, also known as protein kinase B or PKB), which in turn results in the promotion of downstream cellular processes such as cell growth, proliferation, survival, and metabolism.[10,11]

The activation of PI3K signaling has been thought to contribute to tumor growth in humans via three distinct mechanisms: (1) activating point mutations in the gene that encodes the p110α catalytic domain of PI3K (PIK3CA),[10,12−18] (2) the amplification of the PIK3CA gene,[1,19−21] and (3) loss of function of PTEN.[1,22−25] In all three cases, the net result is activation that leads to increased levels of PIP3 production and the promotion of cell growth and survival. PI3K signaling subsequently leads to the activation of downstream targets such as the serine−threonine kinase, PKB, and the mammalian target of rapamycin (mTOR), which integrates signals from growth factors, nutrients, and cellular engergetics to promote cell growth and survival.[26] Since many human cancers have been found to be associated with somatic genetic alterations that result in activation of PI3K signaling, considerable attention has been directed toward targeting PI3K via ATP-competitive small molecule inhibitors, either selectively or in conjuction with mTOR inhibition.[27−29] Several small-molecule inhibitors of both categories have recently been reported, and a number of these are currently undergoing clinical trials, including dual PI3K/mTOR inhibitors such as 2-methyl-2-[4-[3-methyl-2-oxo-8-(quinolin-3-yl)-2,3-dihydroimidazo[4,5-*c*]quinolin-1-yl]phenyl]propionitrile (BEZ235, Novartis),

Received: November 12, 2010
Published: February 18, 2011

dx.doi.org/10.1021/jm1014605 | *J. Med. Chem.* 2011, 54, 1789–1811

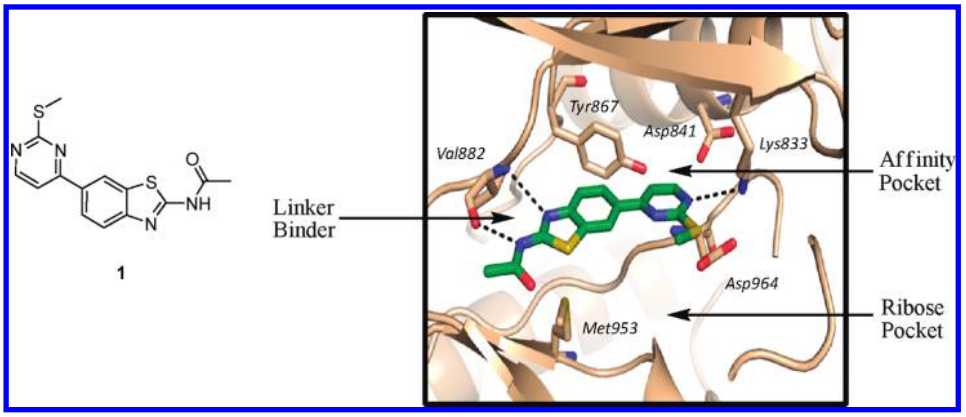

Figure 1. X-ray cocrystal of **1** bound to PI3Kγ.

Scheme 1[a]

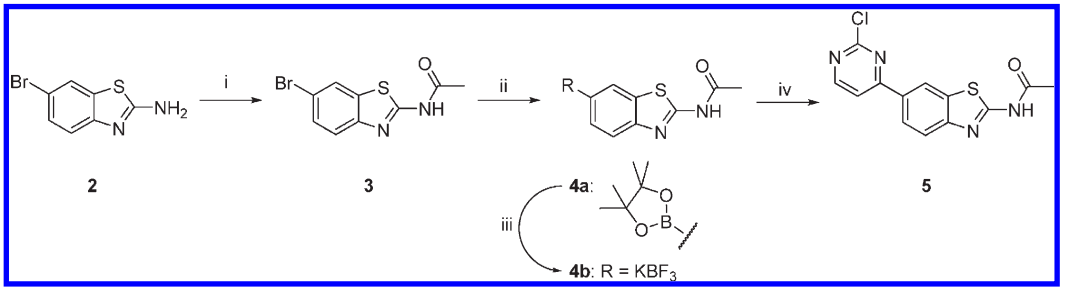

[a] Reagents and conditions: (i) Ac_2O, DMAP, DCM, 0 °C to room temperature, 88%; (ii) bis(pinacolato)diboron, Pd(dppf)Cl_2/DCM, KOAc, DMSO, 100 °C, 91%; (iii) TFE, EtOH, 45 °C; KHF_2, room temperature, 69%; (iv) 2,4-dichloropyrimidine, Pd$(PPh_3)_4$, Na_2CO_3, H_2O, 1,4-dioxane, 95 °C, 85%.

N-(4-(*N*-(3-(3,5-dimethoxyphenylamino)quinoxalin-2-yl)sulfamoyl) phenyl)-3-methoxy-4-methylbenzamide (XL765, Exelixis), and 2,4-difluoro-*N*-{2-(methyloxy)-5-[4-(4-pyridazinyl)-6-quinolinyl]-3-pyridinyl}benzenesulfonamide (GSK2126458, GlaxoSmithKline), as well as selective PI3K inhibitors such as 4-(2-(1*H*-indazol-4-yl)-6-((4-(methylsulfonyl)piperazin-1-yl)methyl)thieno[3,2-*d*] pyrimidin-4-yl)morpholine dimethanesulfonate (GDC-0941, Genentech), 5-[2,6-di(4-morpholinyl)-4-pyrimidinyl]-4-(trifluoromethyl)-2-pyridinamine (BKM120, Novartis), and *N*-(3-(benzo[*c*][1,2,5]thiadiazol-5-ylamino)quinoxalin-2-yl)-4-methylbenzenesulfonamide (XL147, Sanofi/Exelixis).[29−33] Herein, we describe our initial efforts in this field that led to the discovery and optimization of a potent series of benzothiazole PI3K/mTOR dual inhibitors.

We conducted a high-throughput screen and identified **1** as an initial hit. This compound exhibited good PI3Kα enzyme potency (K_i = 53 nM) and thereby served as a suitable starting point for our SAR studies, despite its low mTOR activity (K_i > 25 μM). To guide these efforts, we solved the crystal structure of **1** bound to PI3Kγ, whose structure is likely to closely mimic that of PI3Kα.[34,35] As illustrated in Figure 1, the *N*-acetylbenzothiazole moiety forms two hydrogen bonds with the PI3Kγ residue Val882 of the hinge region. In addition, the pyrimidine ring forms a hydrogen bond with Lys833 and is adjacent to Asp841 and Tyr867 in the "affinity pocket". We postulated that changes to the pyrimidine moiety to engage these three residues might improve potency. Finally, the thiomethyl group extends toward the "ribose pocket", the region of the kinase that is occupied by the ribose moiety of ATP. The crystal structure suggests that this pocket could accommodate significantly larger groups, which may also serve to improve potency.

Table 1. Synthesis of Carbon, Sulfur, Oxygen, and Nitrogen-Linked Analogues

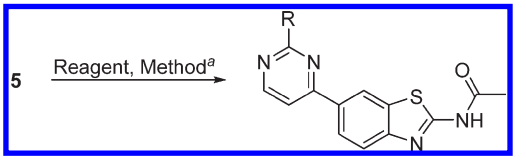

reagent	method[a]	R	compd
PhSH	A	SPh	**6**
BnSH	A	SBn	**7**
PhOH	A	OPh	**8**
BnOH	B	OBn	**9**
$PhNH_2$	A	NHPh	**10**
$BnNH_2$	B	NHBn	**11**
$PhCH_2ZnBr$	C	CH_2Ph	**12**
$PhCH_2CH_2ZnBr$	C	CH_2CH_2Ph	**13**

[a] Method A: NaH, DMF or DMSO, **5**, 13−25%. Method B: **5**, pyridine, 120 °C, microwave irradiation, 300 W, 6−22%. Method C: **5**, Pd$(PPh_3)_4$, THF, 80 °C, 8−11%.

CHEMISTRY

Our first objective was the synthesis of pyrimidine chloride **5**, which was required to make analogues of **1**. The synthesis of **5**

dx.doi.org/10.1021/jm1014605 |*J. Med. Chem.* 2011, 54, 1789–1811

Scheme 2[a]

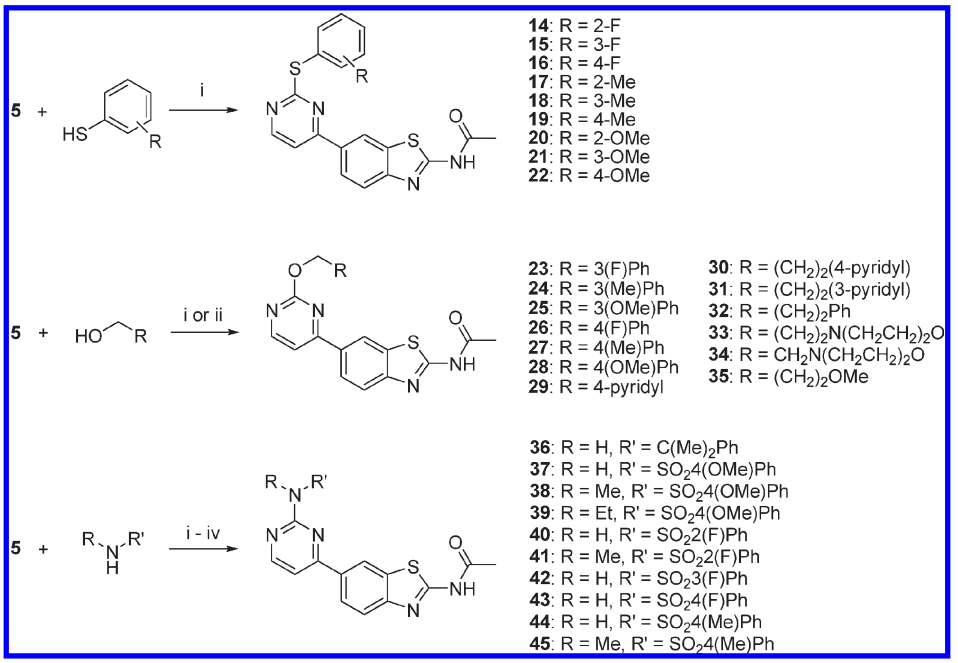

[a] Reagents and conditions: (i) NaH, DMF or DMSO, 12−69%; (ii) pyridine, 120 °C, microwave irradiation, 300 W, 5−22%; (iii) Cs_2CO_3, DMF, 180 °C, microwave irradiation, 180 W, 2%; (iv) NaH, DMF, **5**, $Pd(OAc)_2$, Xantphos, 100 °C, microwave irradiation, 100 W, 16−36%.

began with the acylation of commercially available 2-amino-6-bromobenzothiazole **2** to provide **3** (Scheme 1). Conversion of **3** to boronate **4a**, followed by Suzuki coupling with 2,4-dichloropyrimidine, afforded **5** in three high-yielding steps.[36] In addition, boronic ester **4a** was converted into Molander salt **4b**, which was used for subsequent Suzuki couplings.[37−39]

Compound **5** served as a versatile intermediate for the preparation of several analogues, many of which were made via S_NAr displacement of the pyrimidine chloride. As outlined in Table 1, the sulfur-, oxygen-, and nitrogen-linked phenyl and benzyl analogues (**6**−**11**) were made by base-mediated or microwave-mediated chloride displacement with the corresponding thiols, alcohols, and amines. Carbon-linked analogues **12** and **13** were prepared via Negishi coupling of **5** with benzylzinc bromide and phenethylzinc bromide, respectively.[40] Thiophenyl analogues **14**−**22** were prepared by the reaction of the corresponding sodium thiophenoxides with **5**. Oxygen-linked analogues **23**−**35** were prepared by the reaction of the corresponding alcohols with **5**, again with either base-mediated or microwave-mediated pyrimidine chloride displacement. Finally, nitrogen-linked analogues **36**−**45** were obtained in a similar manner by the reaction of **5** with the corresponding sulfonamides or, in the case of **36**, with cumylamine (Scheme 2).[41] The specific methods used for the synthesis of analogues **14**−**45** are summarized in the Supporting Information.

The syntheses of amide **48** and central ring analogues **51**, **54**, **57**, **60**, and **63** are shown in Scheme 3. Commercially available 2-amino-4-chloropyrimidine **46** was converted to amide **47**, and subsequent Suzuki coupling with boronic ester **4a** provided **48** (Scheme 3A). Sulfonamide **51** was prepared from commercially available 2-chloro-4-iodopyridine **49** via a two-step Suzuki coupling/S_NAr chloride displacement process (Scheme 3B). By contrast, sulfonamide **54** was obtained from commercially available bromide **52** using a two-step sequence in which the sulfonamide formation preceded the Suzuki coupling (Scheme 3C). Compounds **57** (Scheme 3D) and **60** (Scheme 3E) were prepared in a similar manner as **51**, with the routes differing only in the manner in which the sulfonamide was formed. Sulfonamide **57** was prepared via S_NAr chloride displacement of pyrazine **56**, while compound **60** was made by sulfonylation of amine **59** with 4-methoxybenzenesulfonyl chloride. Finally, analogue **63** was prepared from bromide **61** using the sulfonamamide formation/Suzuki coupling sequence that was used to prepare **54** (Scheme 3F).

The preparation of analogue **68** required a longer synthetic sequence, as shown in Scheme 4. Commercially available chloropyridine **64** was treated with diethyl malonate in the presence of sodium hydride to introduce carbon functionality at the 2-position of the pyridine ring. Subsequent decarboxylation under acidic conditions provided methylpyridine **65**.[42] Reduction of the nitro group afforded amine **66**, and then Suzuki coupling with boronic ester **4a** and subsequent sulfonamide formation completed the synthesis of **68**.

Finally, sulfonamide analogues **70**−**82** were all prepared from commercially available bromide **69** in two steps (Table 2). These syntheses involved Suzuki couplings, either with boronic ester **4a** or with Molander salt **4b**, and a sulfonamide formation step, with the sequence of these steps varying from compound to compound. This route provided facile access to compounds in this series, facilitating both the initial SAR studies and subsequent scale-up efforts of larger amounts of material for In Vivo studies.

RESULTS AND DISCUSSION

SAR and Lead Generation. On the basis of the X-ray cocrystal structure of **1**, we replaced the thiomethyl group with thiophenyl (**6**) and thiobenzyl (**7**) groups to see how larger

dx.doi.org/10.1021/jm1014605 |J. Med. Chem. 2011, 54, 1789–1811

Scheme 3[a]

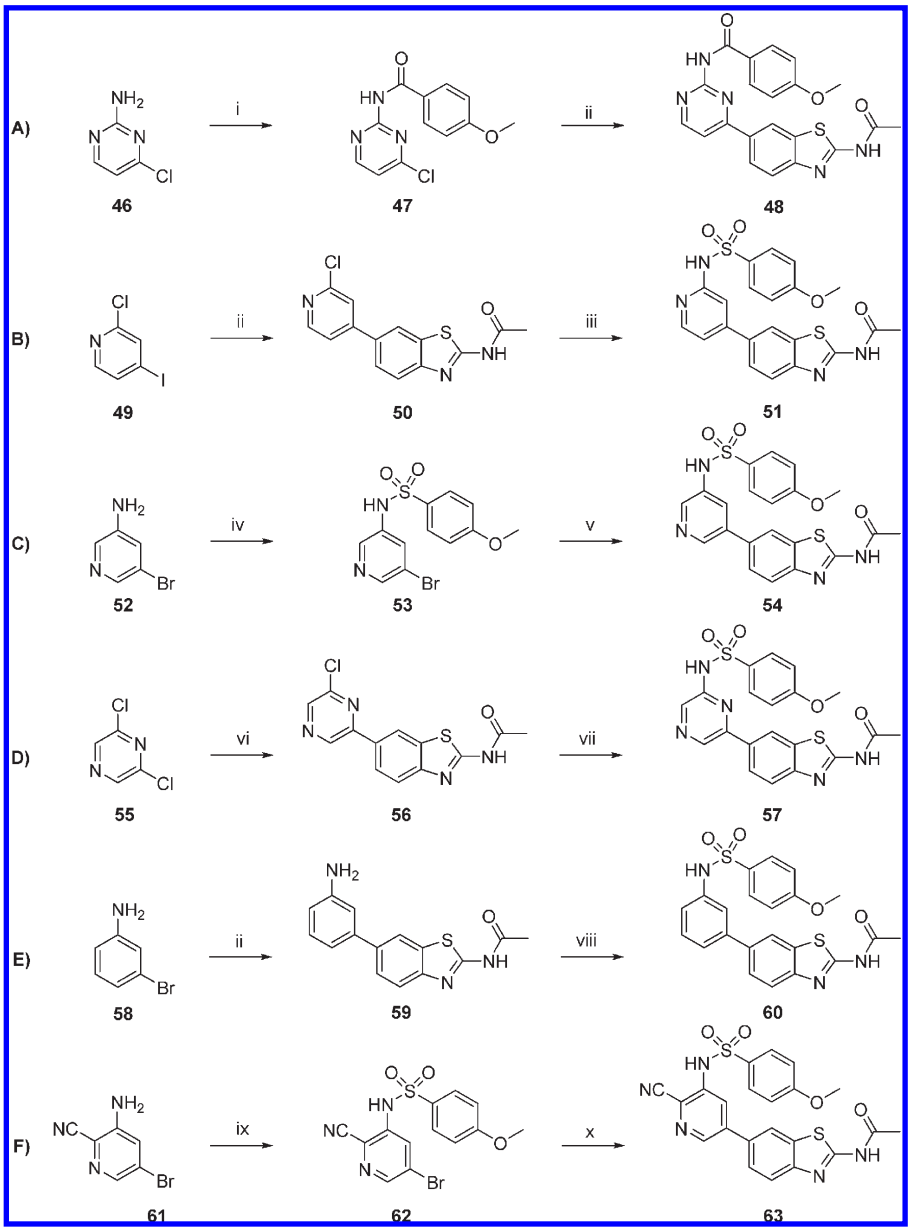

[a] Reagents and conditions: (i) 4-anisoyl chloride, Et_3N, DCM, 5%; (ii) **4a**, $Pd(PPh_3)_4$, Na_2CO_3, H_2O, 1,4-dioxane, 90 °C, 18−32%; (iii) 4-methoxybenzenesulfonamide, NaH, $Pd(OAc)_2$, Xantphos, DMF, 120 °C, microwave irradiation, 100 W, 12%; (iv) 4-methoxybenzenesulfonyl chloride, EtOH, 21%; (v) **4a**, Fibercat, Na_2CO_3, H_2O, 1,4-dioxane, 100 °C, microwave irradiation, 100 W, 16%; (vi) **4a**, $Pd(dppf)Cl_2$, K_2CO_3, H_2O, DME, 90 °C, 62%; (vii) 4-methoxybenzenesulfonamide, NaH, DMSO, 125 °C, 4%; (viii) 4-methoxybenzenesulfonyl chloride, pyridine, pyrrolidine, DCM, 73% (ix) 4-methoxybenzenesulfonyl chloride, LiHMDS, THF, −40 °C to room temperature, 8%; (x) **4a**, $Pd(dppf)Cl_2$, Na_2CO_3, H_2O, DME, 100 °C, 4%.

substituents would affect enzyme potency (Table 3). These changes had a negligible effect on PI3Kα potency, suggesting that larger thioaryl groups could be tolerated in the ribose pocket. Benzyloxy analogue **9** and benzylamine analogue **11** were approximately 2 times less potent than **7**, suggesting that changing the linker atom from sulfur to oxygen or nitrogen had minimal impact on enzyme potency with a benzyl group attached. However, with a phenyl group, the effect of changing the linker atom was more pronounced. While the phenyloxy analogue **8** was about 2 times less potent than **6**, the aniline analogue **10** was over 100 times less potent. Finally, carbon-linked analogues **12** and **13** were at least 10 times less potent than **1**.

Overall, these results reflect the impact of the linking atom on enzyme potency. The sulfur and oxygen atoms would position the benzyl and phenyl groups in the ribose pocket in a manner that would minimize lone-pair interactions between the linking atom and the pyrimidine ring. The comparable potencies of analogues **6**−**9** suggest that all of these analogues adopt similar conformations. However, the nitrogen linking atom of compound **10** would likely adopt a planar conformation relative to the pyrimidine ring and would thereby position the aryl group differently in the ribose pocket.[43] On the basis of the micromolar potency of **10**, this change results in significant steric interference between the aryl group and the ribose pocket. However, the

dx.doi.org/10.1021/jm1014605 |*J. Med. Chem.* 2011, 54, 1789–1811

Scheme 4[a]

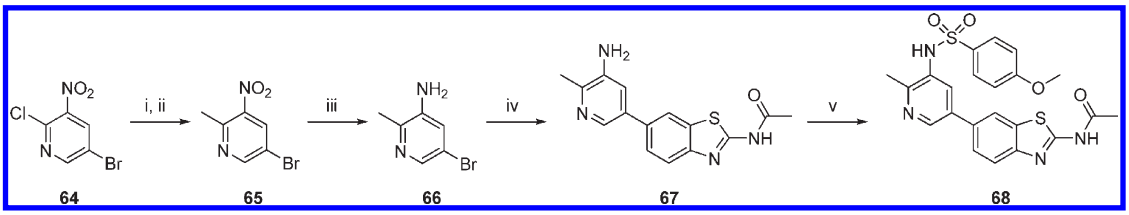

[a] Reagents and conditions: (i) diethyl malonate, NaH, DMF, 40 °C; (ii) HCl, H_2O, 110 °C; (iii) Fe, HOAc, H_2O, 52%; (iv) **4a**, $Pd(dppf)Cl_2$, K_2CO_3, H_2O, DME, 100 °C, 50%; (v) 4-methoxybenzenesulfonyl chloride, DMAP, pyridine, THF, 65 °C, 53%.

Table 2. Synthesis of Sulfonamide Analogues

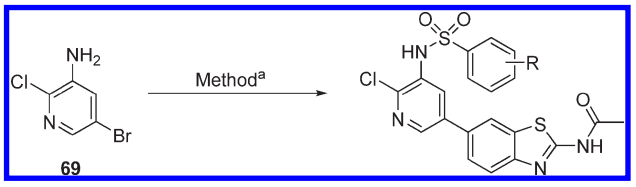

method[a]	R	compd
A	4-OMe	**70**
C	H	**71**
B	2-CF_3	**72**
B	3-CF_3	**73**
C	4-CF_3	**74**
B	2-Cl	**75**
C	3-Cl	**76**
C	4-Cl	**77**
B	3-^{t}Bu	**78**
C	4-^{t}Bu	**79**
B	2-F	**80**
C	3-F	**81**
C	4-F	**82**

[a] Method A: (i) 4-methoxybenzenesulfonyl chloride, pyridine, 110 °C, 49%; (ii) **4a**, Fibercat, Na_2CO_3, H_2O, 1,4-dioxane, 100 °C, 41%. Method B: (i) **69**, LiHMDS, THF, −78 °C; $ArSO_2Cl$, −78 °C to room temp, 45−99%; (ii) **4b**, $Pd(dppf)Cl_2$, Na_2CO_3, H_2O, 1,4-dioxane, 100 °C, 18−62%. Method C: (i) **4a**, $Pd(PPh_3)_4$, K_2CO_3, H_2O, 1,4-dioxane, 100 °C, 33%; (ii) $ArSO_2Cl$, DMAP, THF, pyridine, 8−69%.

addition of the extra methylene unit in benzyl derivative **11** alleviates this steric encumbrance by extending the aryl group further into the ribose pocket, resulting in a significant increase in potency. Finally, the carbon linking atom would orient the aryl groups to minimize steric interactions with the pyrimidine ring. On the basis of the potencies of **12** and **13**, this results in conformations that do not bind well to PI3Kα.

On the basis of the enzyme activity of **6**, we conducted further SAR studies on the thiophenyl moiety of this compound (Table 4). In particular, we examined the effect of fluoro, methyl, and methoxy groups at the 2, 3, and 4 positions. The fluoro and methyl groups had negligible impact on enzyme potency, regardless of their positions (**14**−**16** and **17**−**19**, respectively). However, the larger methoxy group decreased potency at the 2-position (**20**), maintained potency at the 3-position (**21**), and slightly improved potency at the 4-position (**22**). Overall, these results suggest that the phenyl group is surrounded by enough space to tolerate small substituents such as the fluoro or methyl

Table 3. Linker Atom SAR[a]

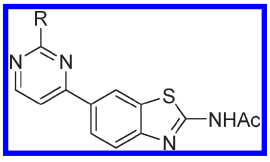

compd	R	PI3Kα K_i (nM)[b]	mTOR IC_{50} (nM)[b]
1	-SMe	53 ± 1	>6000[c]
6	-SPh	40 ± 0.4	>6000[c]
7	-SBn	47 ± 3	>6000
8	-OPh	102 ± 4	>6000
9	-OBn	105 ± 19	>6000
10	-NHPh	6100[c]	>6000[c]
11	-NHBn	85 ± 0.2	>6000
12	-CH_2Ph	605 ± 102	>6000[c]
13	-CH_2CH_2Ph	1010[c]	>6000[c]

[a] See Experimental Methods for assay details. [b] Average of two experiments. [c] Single experiment.

group. However, with the larger methoxy group, the relative potencies of **20** and **22** suggest that there is more room for larger substituents at the 4-position than at the 2-position. In addition, lone pair interactions between the sulfur atom and methoxy group of **20** could change the orientation of the phenyl group in the ribose pocket just enough to result in decreased potency. We also evaluated the compounds listed in Table 7 for their ability to inhibit Akt phosphorylation in U-87 MG cells. However, none of the compounds were potent, as the IC_{50} for all of these compounds was over 1 μM. Given the similar enzyme potencies of **6** and **7**, we did not expect that extensive SAR studies of **7** would lead to dramatically improved enzyme or cellular activities. For this reason, further SAR studies on sulfur-linked analogues were not pursued.

We next examined the optimization of benzyloxypyrimidine **9** (Table 5). Like the sulfur-linked series, we initially examined the effect of a fluoro, methyl, and methoxy group on potency (**23**−**28**). These analogues had enzyme potencies similar to **9** except for **25**, which was about 5 times more potent. However, the cellular activity of all of these compounds in the pAKT cellular assay was also over 1 μM. At this point, it became clear that simple phenyl substituents were unlikely to significantly affect enzyme or cellular potencies and that more significant structural changes would be required.

We replaced the phenyl ring of **9** with a pyridine ring (**29**), a change that had a negligible impact on potency. Likewise, extending the pyridine further out into the ribose pocket (**30**)

dx.doi.org/10.1021/jm1014605 |J. Med. Chem. 2011, 54, 1789–1811

Table 4. Sulfur-Linker SAR[a]

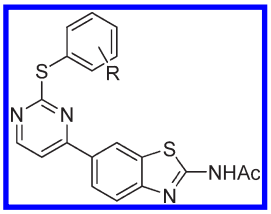

compd	R	PI3Kα K_i (nM)[b]	mTOR IC_{50} (nM)[b]
6	H	40 ± 0.4	>6000[c]
14	2-F	46 ± 5	>6000[c]
15	3-F	31 ± 5	>6000[c]
16	4-F	44 ± 4	>6000[c]
17	2-Me	31 ± 7	>6000[c]
18	3-Me	53 ± 7	>6000[c]
19	4-Me	59 ± 6	>6000[c]
20	2-OMe	144 ± 19	>6000[c]
21	3-OMe	48 ± 3	>6000[c]
22	4-OMe	18 ± 1	3010 ± 1100

[a] See Experimental Methods for assay details. [b] Average of two experiments. [c] Single experiment.

and subsequently shifting the pyridine nitrogen to the 3-position (**31**) had no effect. Interestingly, replacing the pyridine ring with a phenyl ring (**32**) improved potency, albeit only by a factor of 3. However, replacing the pyridine or phenyl ring with a morpholine group (**33**) had no significant impact on potency relative to **9**. Shortening the carbon tether by one unit (**34**) significantly reduced enzyme potency to above 1 μM. Likewise, replacing the aryl or morpholine group of **30**−**33** with a methoxy group (**35**) also reduced potency. The differing potencies of **30**−**35** suggest that both a three-carbon tether and an aryl group (or a similar-shaped substituent like a morpholine group) at the end of this tether are necessary for preserving enzyme potency relative to **9**. This could be the result of π−π stacking or van der Waals interactions at the edge of the ribose pocket. These data do not support the presence of a hydrogen bond in this region, as pyridine **30** and morpholine **33** have similar potencies (100−150 nM) as **9** while **32**, whose phenyl group would not be considered a hydrogen bond donor or acceptor, is more potent. Overall, while these oxygen-linked analogues enabled us to gain a better understanding of the SAR of this series in the ribose pocket, they did not result in any significant improvement in potency relative to **9** (outside of compound **32**) or in any cellular activities with IC_{50} values of less than 1 μM. As a result of these findings and the similar enzyme potencies of oxygen linked analogues **8** and **9**, further SAR studies within the oxygen linked series were not pursued.

We began our optimization of the nitrogen-linked series from benzylamine **11**, the more potent of the two initial nitrogen analogues. Our SAR studies on the sulfur series indicated that aryl substituents were unlikely to significantly improve enzyme potency. Likewise, the data from the oxygen series indicated that extending aryl groups further out into the ribose pocket would not improve potency. Therefore, within this series, we focused initially on the region around the nitrogen atom. Along these lines, we introduced a gem-dimethyl moiety at the benzyl position of **11**, resulting in an improvement in potency of over 3-fold (**36**, Table 6). Introducing a carbonyl at the benzyl position (**48**) resulted in a compound with weak activity (K_i = 3.1 μM). However, replacing this amide group with a sulfonamide (**37**) restored PI3Kα enzyme potency to a similar level compared with **11**. The aryl groups of **11**, **36**, and **37** all have similar spatial orientations in the ribose pocket because of the sp^3 hybridization of the benzyl carbon for compounds **11** and **36** and the sulfonamide sulfur for compound **37**. These similar orientations may account for their similar PI3Kα enzyme potencies. However, the amide functionality of **48** (with an sp^2 hybridized carbon) positions the aryl group differently, a change the data suggest is not well tolerated. In fact, a molecular modeling overlay of **48** with the X-ray cocrystal of **1** showed significant steric interactions between the aryl group and the ribose pocket, which could account for the drop in potency.

The introduction of the sulfonamide group also resulted in a dramatic improvement in mTOR potency, as **37** was the first compound in this paper with an mTOR IC_{50} below 100 nM. In fact, replacing the gem-dimethyl group of **36** with a sulfonamide had a much greater impact on mTOR potency than on PI3Kα potency. The change in mTOR potency between these two compounds is most likely explained by the formation of a hydrogen bond between the mTOR protein and one or both of the sulfonamide oxygens. The similar PI3Kα enzyme potencies of **36** and **37** suggest that such a hydrogen bond is not formed in PI3Kα nor is it necessary for enzyme activity.

While dimethylbenzylamine **36** was more potent than sulfonamide **37** in the PI3Kα enzyme assay, its enzyme-to-cell shift was over 100-fold. By contrast, the enzyme-to-cell shift for **37** was just over 20-fold. For this reason, we sought to optimize **37**, beginning with the introduction of a methyl group (**38**) and an ethyl group (**39**) off the sulfonamide nitrogen. For both of these analogues, a modest increase in enzyme potency was observed. However, what was especially noteworthy among compounds **38** and **39** was the marked improvement in cell potency relative to **37**. The enzyme potency of compound **38** was virtually unchanged, while the cellular potency improved by almost 10-fold. A similar gain in cellular potency was also observed between 2-fluorophenylsulfonamides **40** and **41**, as well as with 4-methylphenylsulfonamides **44** and **45**. In fact, the cellular potency of **41** was over 5 times more potent than **40** despite the fact that the enzyme potencies of these compounds were similar. The improvement in cellular potency for *N*-methyl analogues **38**, **41**, and **45** relative to **37**, **40**, and **44** could be explained by the loss of a hydrogen bond donor, which could allow for better cell permeability.

The incorporation of the sulfonamide moiety was a key discovery in our efforts to optimize the enzyme potency of **1**. This change afforded a number of compounds with enzyme potencies below 100 nM. In addition, the cellular potency and low enzyme to cell shift data for **38** and **45** were especially encouraging, as these were among the most potent compounds prepared thus far.

Because of the improved cellular activity of **45**, we next examined its in vitro and In Vivo pharmacokinetic (PK) profile. Unfortunately, its in vitro clearance was high in both human and rat liver microsomes (579 and >399 (μL/min)/mg, respectively). This high in vitro clearance translated into high clearance (3.7 (L/h)/kg) In Vivo when **45** was administered intravenously (iv) to rats at a dose of 2 mg/kg. Similarly, compound **38** also exhibited high in vitro clearance (>399 (μL/min)/mg in both human and rat liver microsomes) and high In Vivo clearance (4.6 (L/h)/kg in rats). The high In Vivo clearance of **38** and **45** precluded further In Vivo studies with these molecules.

Table 5. Oxygen-Linker SAR[a]

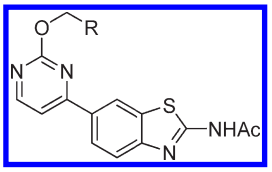

Compound	R	PI3Kα Ki (nM)[b]	mTOR IC_{50} (nM)[b]
9	-Ph	105 ± 19	>6,000
23	-3(F)Ph	61 ± 0.1	>6,000
24	-3(Me)Ph	47 ± 0.1	>6,000[c]
25	-3(OMe)Ph	18 ± 2	>6,000[c]
26	-4(F)Ph	141 ± 16	>6,000
27	-4(Me)Ph	58 ± 0.4	>6,000[c]
28	-4(OMe)Ph	58 ± 7	>6,000[c]
29		128 ± 27	>6,000
30	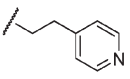	114 ± 4	>6,000[c]
31	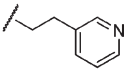	113 ± 6	913[c]
32	-$(CH_2)_2$Ph	32 ± 1	>6,000[c]
33	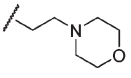	148 ± 45	>6,000[c]
34	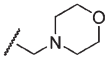	1550 ± 220	ND
35	-$(CH_2)_2$OMe	333 ± 12	ND

[a] See Experimental Methods for assay details. [b] Average of two experiments. [c] Single experiment.

To this point, our SAR studies produced compounds with enzyme potencies under 50 nM and cellular potencies under 400 nM. However, for further In Vivo studies to be pursued, the cellular potencies and In Vivo clearance would have to be improved. To address these issues, we investigated changes to the central pyrimidine ring. In particular, we examined the effect of removing and/or shifting the central ring nitrogens (Table 7). Changing the core from pyrimidine **37** to 2,4-disubstituted pyridine **51** dramatically improved both PI3Kα enzyme and cellular potency. Changing to the isomeric 3,5-disubstituted pyridine **54** improved enzyme potency to single digit nanomolar levels and lowered mTOR activity as well. One reason for the improved enzyme potency of **54** could be the formation of favorable hydrogen bond interactions between the pyridine nitrogen and the Asp841 and Tyr867 residues in the affinity pocket. The introduction of an additional nitrogen (i.e., pyrazine **57**) decreased the enzyme and cellular potencies relative to **54**, while removing all nitrogens from this central ring (**60**) resulted in a further loss of activity, especially against mTOR.

The central ring modifications were key discoveries in our efforts to improve enzyme and cellular potencies. As a result of these changes, we obtained two compounds with single digit enzyme potencies and one compound with cellular activity below 50 nM. We also were able to improve mTOR activity. The PI3Kα and mTOR enzyme potencies of **54** led us to incorporate the 3,5-disubstituted pyridine ring into future analogues.

The next phase of our SAR investigations involved the introduction of substituents at the 2-position of the central pyridine ring. On the basis of the X-ray crystal structure of **1**, we recognized that only small substituents would be tolerated, and this influenced our studies on this portion of the molecule (Table 8). The introduction of cyano, methyl, and chloro groups had minimal effects on PI3Kα and mTOR enzyme potencies. However, the cyano substitution decreased cellular activity significantly while the methyl and chloro groups resulted in a 5- to 20-fold improvement in potency. The subnanomolar enzyme and single-digit nanomolar cellular potencies of **70** were the best for any compound studied in this series to this point. The use of the 2-chloro-3-sulfonamidopyridine moiety in PI3Kα inhibitors has been previously reported.[33,44−47] However, the combination of this moiety with the benzothiazole hinge binder described in this work represents a novel scaffold for a PI3Kα inhibitor. Having optimized the in vitro enzyme and cellular activities, we focused on improving the PK properties of these molecules.

We first evaluated the in vitro clearance of **70** in human and rat liver microsomes (HLM and RLM) and found the latter to be high, precluding further studies with this molecule (Table 9). The RLM data for phenylsulfonamide **71** were high as well. Therefore, we pursued SAR studies on the phenylsulfonamide portion of the molecule, with the goal of achieving HLM and RLM clearances below 50 (μL/min)/mg.

All of the analogues shown in Table 9 exhibited similar enzyme and cellular potencies, indicating that there is enough room in the ribose pocket to accommodate small groups, regardless of their position on the phenyl ring (not unlike the sulfur- and oxygen-linked analogues discussed earlier). In addition, these analogues were all potent mTOR inhibitors. However, the HLM and RLM data indicated that metabolic stability differed significantly. Compounds substituted at the 4-position with electron withdrawing substituents exhibited low in vitro clearance (values below 20 (μL/min)/mg), while the corresponding 2- and 3-substituted derivatives exhibited higher clearance values, as evidenced by the chloro, fluoro, and trifluoromethyl compounds. These data suggested that the phenyl 4-position was readily metabolized and that substitution at this position with an electron withdrawing group was critical for obtaining metabolic stability. We identified **73**, **74**, **77**, and **82** as the only compounds with HLM and RLM values below 50 (μL/min)/mg.

In order to better understand the potency of the compounds in Table 9, we next examined an X-ray cocrystal of compound **82** bound to PI3Kγ (Figure 2). The X-ray cocrystal structure of **82** overlaps quite closely with **1**, with little movement of the protein observed. As observed with compound **1**, the *N*-acetylbenzothiazole forms two hydrogen bonds with Val882 (Figure 2A). However, the hydrogen bond with the Lys833 residue was not retained, despite the proximity of the sulfonamide nitrogen

dx.doi.org/10.1021/jm1014605 |*J. Med. Chem.* 2011, 54, 1789–1811

Table 6. Nitrogen-Linker SAR[a]

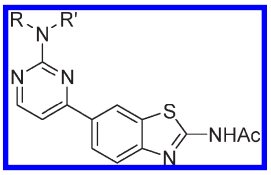

Compound	R	R'	PI3Kα Ki (nM)[b]	pAKT IC_{50} (nM)	mTOR IC_{50} (nM)[b]
11	H	-Bn	85 ± 0.2	> 5,000[c]	>6,000
36	H	$-C(Me)_2Ph$	24 ± 5	2,800[c]	>6,000
48	H	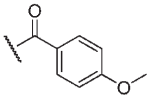	3130 ± 780	ND	>6,000[c]
37	H	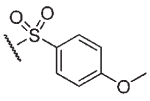	117 ± 20	2,500[c]	57[c]
38	Me	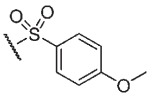	76 ± 10	336 ± 27[b]	285 ± 51
39	Et	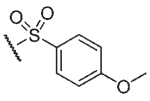	62 ± 0.4	305[c]	262 ± 29
40	H	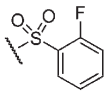	41 ± 1	4,010[c]	45 ± 20
41	Me	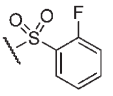	65 ± 13	676[c]	>6,000[c]
42	H	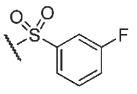	84 ± 4	> 5,000[c]	47[c]
43	H	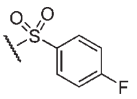	826 ± 81	> 5,000[c]	719[c]
44	H	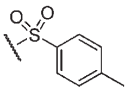	82 ± 0.5	1,260[c]	65 ± 12
45	Me	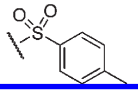	38 ± 1	334 ± 16[b]	269 ± 111

[a] See Experimental Methods for assay details. [b] Average of two experiments. [c] Single experiment.

(3.6 Å) and oxygen atoms (3.3 Å).[48] The loss of this hydrogen bond was offset with the gain of two hydrogen bonds formed via an ordered water molecule located between the central chloropyridine ring nitrogen and the Tyr867 and Asp841 residues. These additional hydrogen bonds help explain the gain in enzyme potency achieved with the chloropyridine central ring. In addition,

dx.doi.org/10.1021/jm1014605 |J. Med. Chem. 2011, 54, 1789–1811

Table 7. Central Ring SAR[a]

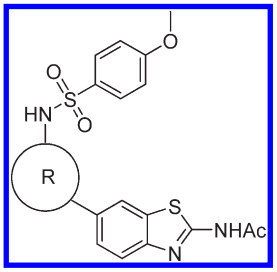

Compound	R	PI3Kα Ki (nM)[b]	pAKT IC_{50} (nM)	mTOR IC_{50} (nM)[b]
37	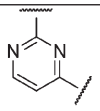	117 ± 20	2,500[c]	57[c]
51	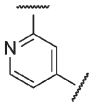	13 ± 1	33 ± 3[b]	29 ± 17
54	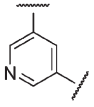	1.6 ± 0.1	103 ± 54[b]	11 ± 1
57	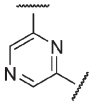	9 ± 1	739[c]	15 ± 2
60	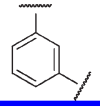	48 ± 2	1,160[c]	1,500 ± 600

[a] See Experimental Methods for assay details. [b] Average of two experiments. [c] Single experiment.

the space-filling model indicates that the arylsulfonamide portion in the ribose pocket has enough space around it to accommodate various substituents (e.g., trifluoromethyl, chloro, and *tert*-butyl) at the 2-, 3-, and 4-positions (Figure 2B). This explains the relatively flat SAR exhibited by the arylsulfonamides (Table 9), as well as by the sulfur analogues (Table 4) and oxygen analogues (Table 5). It also confirms our earlier hypothesis that the ribose pocket would be able to accommodate groups significantly larger than the thiomethyl moiety of **1**. By contrast, the pyridine chloro group of **82** fits into a narrow pocket, confirming (based on the X-ray cocrystal structure of **1**) that only small groups would be tolerated at this position (Figure 2C).

In addition to being a potent dual PI3Kα/mTOR inhibitor, compound **82** was also a potent inhibitor of the other class I PI3K isoforms PI3Kβ (K_i = 2.0 nM), PI3Kγ (K_i = 4.7 nM), and PI3Kδ (K_i = 1.2 nM). The inhibition of cell proliferation by this compound was determined using an ATP-based cell viability assay in PTEN-null U-87 MG glioblastoma and PTEN-null PC-3 prostate carcinoma cell lines. Sulfonamide **82** potently inhibited cell proliferation in both cell lines, exhibiting IC_{50} values of 68 nM (U-87 MG) and 47 nM (PC-3).

Its selectivity against selected members of phosphatidylinositol kinase-related kinases (PIKK) was also examined. Compound **82** was a potent inhibitor of the class III PI3K, hVPS34 (K_i = 31 nM), and DNA-PK (IC_{50} = 3 nM), suggesting that **82** could be considered a pan inhibitor of class I PI3K's with limited selectivity over closely related PIKK's. The selectivity of compound **82** against a panel of over 350 protein and lipid kinases, including class I PI3Ks, was examined using the AMBIT KINOMEscan platform.[49] In this panel, the competitive binding of **82** was measured as a percentage of control (POC) at 1 μM. This compound demonstrated affinity against class I PI3Ks (POC = 0−1%), a finding consistent with the enzyme data mentioned above. However, it exhibited moderate activity (POC = 25−30%) against only two other kinases (CDKL2 and MLCK). For all other kinases assayed, no competitive binding by **82** was observed.[50]

In Vivo Studies. We also evaluated the In Vivo PK profile of this compound. When **82** was administered intravenously (iv) to rats, it exhibited a low clearance (0.007 (L/h)/kg), a low volume of distribution (0.17 L/kg), and a long half-life (19 h). The AUC exposure was 0.32 mg·h/mL. When given orally to rats, it exhibited a bioavailability of 103%.[51] The ability of this compound to inhibit HGF-stimulated PI3K signaling was evaluated in a mouse liver pharmacodynamic (PD) assay. Compound **82** was administered to mice at dosages ranging from 0.03 to 3 mg/kg. Human HGF was injected iv 3 h postdose to induce PI3K-dependent Akt phosphorylation in the liver. Compound **82** induced significant suppression of PI3K signaling, as indicated by a dose-dependent decrease in phosphorylated Akt (p-Akt) at

dx.doi.org/10.1021/jm1014605 |J. Med. Chem. 2011, 54, 1789–1811

Table 8. Central Ring Substitution SAR[a]

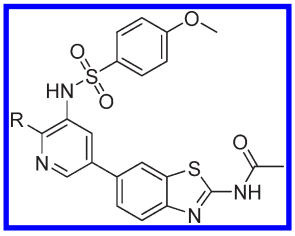

compd	R	PI3Kα K_i (nM)[b]	pAKT IC_{50} (nM)[c]	mTOR IC_{50} (nM)[b]
54	H	1.6 ± 0.1	103 ± 54[b]	11 ± 1
63	CN	1.4 ± 0.1	757[c]	1.6 ± 0.4
68	Me	1.2 ± 0.1	18[c]	6.0 ± 0.4
70	Cl	<1.0	5[c]	2.1 ± 1.0

[a] See Experimental Methods for assay details. [b] Average of two experiments. [c] Single experiment.

Ser473 (Figure 3A). The EC_{50} was found to be 399 ng/mL.[52] In addition, in a time course liver study at 3 mg/kg, **82** maximally inhibited Akt phosphorylation 1 h after dosing and demonstrated significant inhibition for 24 h (Figure 3B). Compound **82** appeared rapidly in plasma with a C_{1h} of 2000 ng/mL and reached a C_{max} of ~3000 ng/mL at 3−8 h.

We next evaluated whether **82** could inhibit tumor growth in established mouse xenograft models. In mice bearing U87-MG (PTEN null) glioblastoma xenografts,[53,54] treatment with this compound, administered orally QD, caused a dose-dependent reduction in tumor growth with an ED_{50} of 0.26 mg/kg (Figure 4A). A similar dose dependency was observed in nude mice bearing A549 (KRAS mutant) lung adenocarcinoma[55,56] and HCT116[18,57] (KRAS and PI3Kα mutant) colon adenocarcinoma xenograft models (Figure 4B and Figure 4C). In all tumor xenograft studies, sulfonamide **82** was well tolerated in terms of its effect on body weight. In only one instance (the 10 mg/kg arm of the HCT116 xenograft study) did the body weight drop below 90% of the starting body weight over the course of the study. These data suggest that compound **82** could potentially inhibit tumor growth against a wide range of tumors with different genetic backgrounds and that its efficacy may not be restricted to those tumors that are caused by a specific pathway mutation or mechanism of activation.

In conclusion, we have discovered and developed a novel series of potent PI3K/mTOR inhibitors from an initial hit, compound **1**. Extensive SAR studies resulted in the discovery of sulfonamide **45**. However, high in vitro and In Vivo clearance necessitated changes to the central pyrimidine ring. This led to the discovery of chloropyridine **70** and, after aryl sulfonamide SAR studies focused on optimizing in vitro clearance, compound **82**. This compound was the most potent analogue prepared in this series in terms of enzyme and cellular potencies. In addition, it also proved to be efficacious when tested in a liver PD assay and three distinct xenograft models. The biological profile of this molecule validated the benzothiazole series as a means of inhibiting tumor growth In Vivo by targeting PI3Kα and mTOR.

EXPERIMENTAL METHODS

Chemistry. All reactions were conducted in a well-ventilated fume hood under N_2 using a Teflon-coated magnetic stirbar at the temperature indicated. Reactions run at elevated temperature were run in an oil bath at the temperature indicated. Microwave reactions were run in a CEM Discover microwave equipped with PowerMAX feature using the settings described below. All solvents and reagents obtained from commercial sources were used without further purification. Removal of solvents was conducted by using a rotary evaporator, and residual solvent was removed from nonvolatile compounds using a vacuum manifold maintained at approximately 1 Torr. All yields reported are isolated yields.

Analytical TLC was performed with EMD 0.25 mm silica gel 60 plates with a 254 nm fluorescent indicator. Plates were developed in a covered chamber and visualized with ultraviolet light. Flash chromatography refers to column chromatography as described by Still using EMD silica gel 60, 230−400 mesh, as the stationary phase.[58] Where noted, ISCO purification refers to a Teledyne ISCO purification system using RediSep columns in the size noted as well as the solvent system and gradients noted.

^{1}H NMR spectra were obtained on a Bruker BioSpin GmbH magnetic resonance spectrometer. ^{1}H NMR spectra are reported as chemical shifts in parts per million (ppm) relative to an internal solvent reference. Peak multiplicity abbreviations are as follows: s (singlet), br s (broad singlet), d (doublet), dd (doublet of doublets), t (triplet), q (quartet), quin (quintet), and m (multiplet).

Analytical HPLC and mass spectrometry were conducted using a reverse-phase Agilent 1100 series HPLC−mass spectrometer. Purities for final compounds were measured using UV detection at 254 nm and are ≥95.0% unless otherwise noted. A detailed description of the HPLC methods that were used for analyzing final compounds is included in the Supporting Information. Elemental analyses (% C, % H, % N) were obtained from Atlantic Microlab, Inc. in Norcross, GA.

***N*-(6-Bromobenzo[*d*]thiazol-2-yl)acetamide (3).** 6-Bromobenzo[*d*]thiazol-2-amine (51.08 g, 223 mmol) was suspended in DCM (800 mL), and DMAP (30.71 g, 251 mmol) was added. The mixture was cooled in an ice−water bath under N_2, and acetic anhydride (23.0 mL, 244 mmol) was added. The mixture was allowed to slowly warm to room temperature while being stirred overnight under N_2. The mixture was treated with 10% HCl (375 mL), and the layers were separated. The organic phase was filtered, and the solid was washed with DCM. The aqueous phase was filtered separately, and the solid collected from this filtration was washed with water and then collected and combined with the solid collected from the filtration of the organic phase. The aqueous phase was extracted with 10:1 DCM/MeOH (300 mL, 200 mL, 150 mL). These organic extracts were combined with the filtrate from the filtration of the organic phase and concentrated. The concentrate was treated with Et_2O and filtered. This solid was washed with Et_2O and set aside. The first batch of solid collected (from the separate filtrations of the organic phase and aqueous phase above) was also treated with Et_2O and filtered. This solid was washed with Et_2O, DCM, and Et_2O and then combined with the other batch of solid. The filtrate from this last filtration was concentrated, treated with Et_2O, and filtered. The solid from this last filtration was washed with Et_2O and then combined with all of the other collected solids to afford **3** (59.97 g, 89% purity, 88% yield). MS (ESI pos ion) *m/z*: 271 ($M + H^+$, ^{79}Br), 273 ($M + H^+$, ^{81}Br). ^{1}H NMR (400 MHz, $CDCl_3$): 12.41 (s, 1H), 8.23 (d, *J* = 2.0 Hz, 1H), 7.66 (d, *J* = 8.5 Hz, 1H), 7.56 (m, 1H), 2.21 (s, 3H).

***N*-(6-(4,4,5,5-Tetramethyl-1,3,2-dioxaborolan-2-yl)benzo[*d*]thiazol-2-yl)acetamide (4a).** *N*-(6-Bromobenzo[*d*]thiazol-2-yl)-acetamide (59.97 g, 221 mmol) and 4,4,5,5-tetramethyl-2-(4,4,5,5-tetramethyl-1,3,2-dioxaborolan-2-yl)-1,3,2-dioxaborolane (76.58 g, 302 mmol) were suspended in DMSO. KOAc (55.8 mL, 893 mmol) was added, followed by more DMSO. The total amount of DMSO used was 650 mL. Then 1,1′-bis(diphenylphosphino)ferrocenepalladium(II) dichloride dichloromethane complex (12.34 g, 16.9 mmol) was added, followed by a DMSO (6 mL) rinse. The flask was placed in a preheated oil bath (90 °C),

Table 9. Phenylsulfonamide SAR[a]

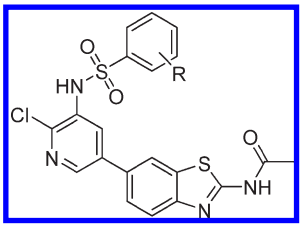

compd	R	PI3Kα K_i (nM)[b]	pAKT IC_{50} (nM)[c]	HLM/RLM ((μL/min)/mg)[c]	mTOR IC_{50} (nM)[b]
70	4-OMe	<1.0	5	42/>399	2.1 ± 1.0
71	H	1.4 ± 0.1	5 ± 1[b]	<14/>399	<1.0
72	2-CF_3	<1.0	8	<14/500	<1.0
73	3-CF_3	<1.0	12	17/36	<1.0
74	4-CF_3	<1.0	19	<14/<14	1.6 ± 1.0
75	2-Cl	<1.0	4.9 ± 0.3[b]	<14/>399	<1.0
76	3-Cl	<1.0	12	16/>399	<1.0
77	4-Cl	<1.0	8.7 ± 0.9[b]	<14/<14	<1.0
78	3-^{t}Bu	<1.0	13	83/610	2.1 ± 0.9
79	4-^{t}Bu	<1.0	7	135/460	2.1 ± 0.3
80	2-F	<1.0	9	<14/320	1.1 ± 0.6
81	3-F	1.1 ± 0.5	13	<14/>399	2.3 ± 0.9
82	4-F	1.2 ± 0.9	6.3 ± 6.5[b]	<14/<20	2.0 ± 4.8

[a] See Experimental Methods for assay details. [b] Average of at least two experiments. [c] Single experiment except where noted.

and the mixture was stirred under argon. After 2 h and 20 min, the mixture was allowed to cool to room temperature and filtered through a pad of Celite, which was then washed with MeOH. The filtrate was partially concentrated and partitioned between H_2O (1000 mL) and DCM (550 mL). The layers were separated, and the aqueous phase was extracted with DCM (3 × 450 mL). The organic extracts were combined and divided into two portions of approximately 1 L each. The first portion was washed with brine (400 mL). The layers were separated, and the aqueous phase was extracted with DCM (2 × 400 mL). These organic phases were combined and set aside. The second portion was combined with these organic extracts. These combined organic phases were dried over Na_2SO_4, filtered, and concentrated. The resultant solid was treated with Et_2O and filtered. The solid was washed with Et_2O and EtOAc, and the filtrate was set aside. The solid was also washed with MeOH and again with EtOAc. The filtrates from both filtrations were combined, concentrated, and purified on silica gel (DCM → 50:1 → 20:1 DCM/MeOH). The fractions with product were collected, concentrated, treated with Et_2O, and filtered. The solid was collected and set aside. The filtrate was concentrated and treated with Et_2O and filtered, and the resulting solid was washed with Et_2O and hexanes. This solid was combined with the solid from the first filtration. The filtrate from this second filtration was concentrated again. This was treated with 1:1 hexanes/Et_2O and filtered. The solid was washed with 1:1 hexanes/Et_2O. This time, the filtrate was concentrated while the solid from this filtration was discarded. This filtrate was combined with the solid collected from the first two filtrations, concentrated, washed with hexanes, and dried to afford **4a** (73.2 g, 88% purity, 91% yield). MS (ESI pos ion) m/z: 319 ($M + H^+$). ^{1}H NMR (400 MHz, $CDCl_3$, δ): 10.44 (br s, 1H), 8.32 (s, 1H), 7.90 (d, J = 8.02 Hz, 1H), 7.76 (d, J = 8.22 Hz, 1H), 2.31 (s, 3H), 1.38 (s, 12H).

Potassium *N*-(6-(Trifluoroboryl)benzo[*d*]thiazol-2-yl)-acetamide (4b). A 125 mL polytetrafluoroethylene (PTFE) beaker was charged with **4a** (4.00 g, 12.6 mmol), 75 mL of EtOH, 25 mL of TFEm and a stir bar. The slurry was sonicated and heated using a 45 °C H_2O bath until a clear solution was apparent. The solution was treated with potassium fluoride hydrofluoride (2.45 g, 31.4 mmol) and stirred at room temperature for 24 h. The precipitate that formed was collected using a 0.22 μm PTFE membrane. The solids were washed with EtOH (2 × 25 mL), H_2O (2 × 25 mL), and EtOH (1 × 25 mL). The solids were dried under a stream of N_2 and then at 60 °C and <1 mmHg for 48 h to afford **4b** (2.60 g, 69.4% yield). ^{1}H NMR (400 MHz, DMF, δ): 2.28 (s, 3 H), 7.50 (d, J = 7.43 Hz, 1H), 7.58 (d, J = 8.02 Hz, 1H), 7.94 (s, 1H), 11.99 (br s, 1H). ^{13}C NMR (101 MHz, DMF, δ): 22.66, 118.97, 123.6, 130.21, 130.85, 147.24, 156.21, 162.58, 169.17. ^{19}F NMR (376 MHz, DMF, ref = $CFCl_3$ = 0.00, δ): −140.19 (s, 3 F). Anal. Calcd for ($C_9H_7BF_3KN_2OS \cdot 0.7H_2O$) C, H, N.

***N*-(6-(2-Chloropyrimidin-4-yl)benzo[*d*]thiazol-2-yl)-acetamide (5).** 2,4-Dichloropyrimidine (10.31 g, 69.20 mmol), *N*-(6-(4,4,5,5-tetramethyl-1,3,2-dioxaborolan-2-yl)benzo[*d*]thiazol-2-yl)acetamide (28.52 g, 89.63 mmol), and $Pd(PPh_3)_4$ (6.052 g, 5.237 mmol) were suspended in 1,4-dioxane (300 mL), and aqueous Na_2CO_3 (2.0 M, 70 mL, 140 mmol) was added. Argon was bubbled through the solution for about 1 min, and then the flask was fitted with a reflux condenser and placed in a preheated oil bath (~95 °C) and stirred under argon overnight. The mixture was cooled to room temperature, and the liquid was decanted. The residual solid was treated with 1:1 DCM/MeOH and filtered through a pad of Celite. This pad was washed with 1:1 DCM/MeOH as well as with some DMF. This filtrate was concentrated, combined with the decanted material, and concentrated again. The concentrated material was treated with DCM and filtered. The solid was washed with DCM, collected, and dried under high vacuum to afford **5** (17.89 g, 85% yield). MS (ESI pos ion) m/z: 305 ($M + H^+$). ^{1}H NMR (400 MHz, DMSO-d_6, δ): 12.58 (s, 1H), 8.87 (s, 1H), 8.82 (d, J = 5.02 Hz, 1H), 8.28 (d, J = 8.53 Hz, 1H), 8.19 (d, J = 5.52 Hz, 1H), 7.87 (d, J = 8.53 Hz, 1H), 2.23 (s, 3H).

Procedure for the Synthesis of 6−8, 10, 14−22, 24−30, and 37−39. *N*-(6-(2-(Phenylthio)pyrimidin-4-yl)benzo[*d*]thiazol-2-yl)acetamide (6). Thiophenol (106.1 mg, 0.963 mmol) was dissolved in DMF (1.0 mL), and sodium hydride (67 mg, 60% in mineral oil, 1.7 mmol) was added. The mixture was stirred under N_2 at room temperature for 1 h, and then **5** (50.4 mg, 0.165 mmol) was added. The mixture was stirred at room temperature for 2.5 h and then was treated with

dx.doi.org/10.1021/jm1014605 |*J. Med. Chem.* 2011, 54, 1789–1811

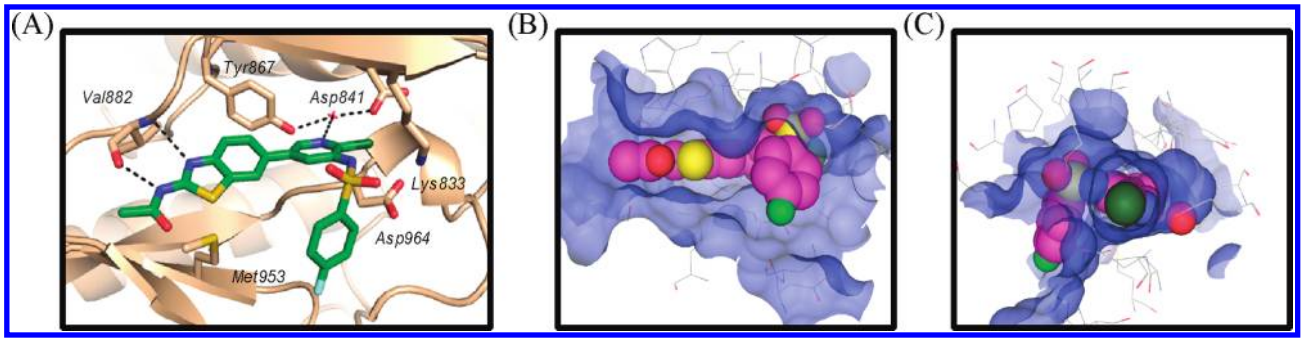

Figure 2. X-ray cocrystal of **82** bound to PI3Kγ. Parts A and B are from a similar vantage point, while part C views the molecule down the C−Cl bond of the chloropyridine central ring.

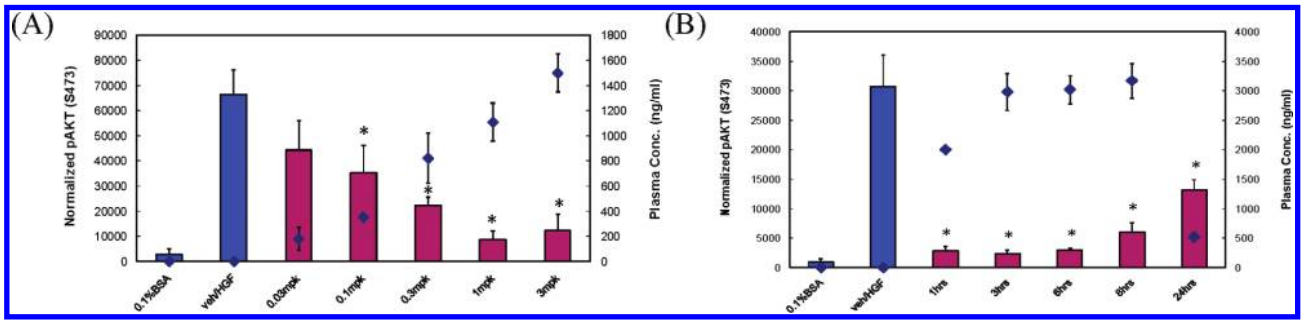

Figure 3. Effect of compound **82** on HGF-mediated AKT phosphorylation (A) at 3 h postdose and (B) in a time course study at 3 mg/kg. Bars represent the mean ± standard deviation ($n = 3$). Diamonds represent mean plasma concentration. Asterisk denotes (A) $p < 0.05$ and (B) $p < 0.001$ compared with the vehicle (HGF) group.

H_2O and saturated $NaHCO_3$. The aqueous phase was extracted with DCM, and the organic extracts were combined, concentrated, treated with MeOH and DCM, and filtered. The filtrate was concentrated and the crude material was purified on HPLC (10% → 95% MeCN/H_2O with 0.1% TFA over 28 min) to afford **6** (16.0 mg, 25% yield). MS (ESI pos ion) m/z: 379 ($M + H^+$). ^{1}H NMR (400 MHz, DMSO-d_6, δ): 12.55 (s, 1H), 8.67−8.62 (m, 2H), 8.10 (d, J = 8.53 Hz, 1H), 7.84 (d, J = 5.02 Hz, 1H), 7.79 (d, J = 8.53 Hz, 1H), 7.69 (dd, J = 6.02, 2.51 Hz, 2H), 7.56−7.51 (m, 3H), 2.23 (s, 3H).

***N*-(6-(2-(Benzylthio)pyrimidin-4-yl)benzo[*d*]thiazol-2-yl) acetamide (7).** Using benzylthiol and following the procedure used to prepare **6** gave **7** in 13% yield. MS (ESI pos ion) m/z: 393 ($M + H^+$). ^{1}H NMR (400 MHz, DMSO-d_6, δ): 12.50 (s, 1H), 8.85 (s, 1H), 8.68 (d, J = 5.0 Hz, 1H), 8.26 (d, J = 8.5 Hz, 1H), 7.84 (m, 2H), 7.49 (d, J = 7.0 Hz, 2H), 7.32 (t, J = 7.3 Hz, 2H), 7.25 (t, J = 7.3 Hz, 1H), 4.54 (s, 2H), 2.23 (s, 3H).

***N*-(6-(2-Phenoxypyrimidin-4-yl)benzo[*d*]thiazol-2-yl)acetamide (8).** Using phenol and following the procedure used to prepare **6** gave **8** in 13% yield. MS (ESI pos ion) m/z: 363 ($M + H^+$). ^{1}H NMR (400 MHz, DMSO-d_6, δ): 12.54 (s, 1H), 8.79 (s, 1H), 8.67 (d, J = 5.52 Hz, 1H), 8.19 (d, J = 8.53 Hz, 1H), 7.88 (d, J = 5.02 Hz, 1H), 7.84 (d, J = 8.53 Hz, 1H), 7.50−7.44 (m, 2H), 7.32−7.26 (m, 3H), 2.23 (s, 3H).

***N*-(6-(2-(Phenylamino)pyrimidin-4-yl)benzo[*d*]thiazol-2-yl) acetamide (10).** Using aniline and DMSO and following the procedure used to prepare **6** gave **10** in 21% yield. This analogue was purified by washing the crude material with Et_2O and DCM. MS (ESI pos ion) m/z: 362 ($M + H^+$). ^{1}H NMR (400 MHz, DMSO-d_6, δ): 2.17 (s, 3H), 7.35 (d, J = 5.28 Hz, 1H), 7.54−7.66 (m, 5H), 7.74 (d, J = 8.61 Hz, 1H), 8.20 (d, J = 6.85 Hz, 1H), 8.25 (d, J = 8.61 Hz, 1H), 8.78 (s, 1H).

***N*-(6-(2-(2-Fluorophenylthio)pyrimidin-4-yl)benzo[*d*]thiazol-2-yl)acetamide (14).** Using 2-fluorothiophenol and following the procedure used to prepare **6** gave **14** in 25% yield. MS (ESI pos ion) m/z: 397 ($M + H^+$). ^{1}H NMR (400 MHz, DMSO-d_6, δ): 12.52 (br s, 1H), 8.66−8.59 (m, 2H), 8.06 (d, J = 8.53 Hz, 1H), 7.86 (d, J = 5.02 Hz, 1H), 7.82−7.80 (m, 2H), 7.65 (q, J = 6.86 Hz, 1H), 7.45 (t, J = 8.53 Hz, 1H), 7.36 (t, J = 7.28 Hz, 1H), 2.23 (s, 3 H).

***N*-(6-(2-(3-Fluorophenylthio)pyrimidin-4-yl)benzo[*d*]thiazol-2-yl)acetamide (15).** Using 3-fluorothiophenol and following the procedure used to prepare **6** gave **15** in 42% yield. MS (ESI pos ion) m/z: 397 ($M + H^+$). ^{1}H NMR (400 MHz, DMSO-d_6, δ): 12.53 (s, 1H), 8.70−8.64 (m, 2H), 8.11 (d, J = 8.53 Hz, 1H), 7.87 (d, J = 5.02 Hz, 1H), 7.81 (d, J = 8.53 Hz, 1H), 7.64−7.51 (m, 3H), 7.39 (t, J = 8.28 Hz, 1H), 2.23 (s, 3H).

***N*-(6-(2-(4-Fluorophenylthio)pyrimidin-4-yl)benzo[*d*]thiazol-2-yl)acetamide (16).** Using 4-fluorothiophenol and following the procedure used to prepare **6** gave **16** in 34% yield. MS (ESI pos ion) m/z: 397 ($M + H^+$). ^{1}H NMR (400 MHz, DMSO-d_6, δ): 12.50 (br s, 1H), 8.68−8.61 (m, 2H), 8.09 (d, J = 8.53 Hz, 1H), 7.84 (d, J = 5.52 Hz, 1H), 7.80 (d, J = 8.53 Hz, 1H), 7.76−7.69 (m, 2H), 7.38 (t, J = 8.78 Hz, 2H), 2.23 (s, 3H).

***N*-(6-(2-(2-Methylphenylthio)pyrimidin-4-yl)benzo[*d*]thiazol-2-yl)acetamide (17).** Using 2-methylthiophenol and following the procedure used to prepare **6** gave **17** in 25% yield. MS (ESI pos ion) m/z: 393 ($M + H^+$). ^{1}H NMR (400 MHz, DMSO-d_6, δ): 12.53 (s, 1H), 8.64−8.60 (m, 2H), 8.07 (dd, J = 8.61, 1.76 Hz, 1H), 7.82 (d, J = 5.48 Hz, 1H), 7.78 (d, J = 8.61 Hz, 1H), 7.64 (d, J = 7.43 Hz, 1H), 7.48−7.44 (m, 2H), 7.35−7.29 (m, 1H), 2.38 (s, 3H), 2.23 (s, 3H).

***N*-(6-(2-(3-Methylphenylthio)pyrimidin-4-yl)benzo[*d*]thiazol-2-yl)acetamide (18).** Using 3-methylthiophenol and following the procedure used to prepare **6** gave **18** in 29% yield. MS (ESI pos ion) m/z: 393 ($M + H^+$). ^{1}H NMR (400 MHz, DMSO-d_6, δ): 12.53 (s, 1H), 8.67 (s, 1H), 8.64 (d, J = 5.52 Hz, 1H), 8.11 (d, J = 8.53 Hz, 1H), 7.84 (d, J = 5.52 Hz, 1H), 7.80 (d, J = 9.03 Hz, 1H), 7.54 (s, 1H), 7.49−7.45 (m, 1H), 7.41 (t, J = 7.53 Hz, 1H), 7.36−7.31 (m, 1H), 2.39 (s, 3H), 2.23 (s, 3H).

dx.doi.org/10.1021/jm1014605 |*J. Med. Chem.* 2011, 54, 1789–1811

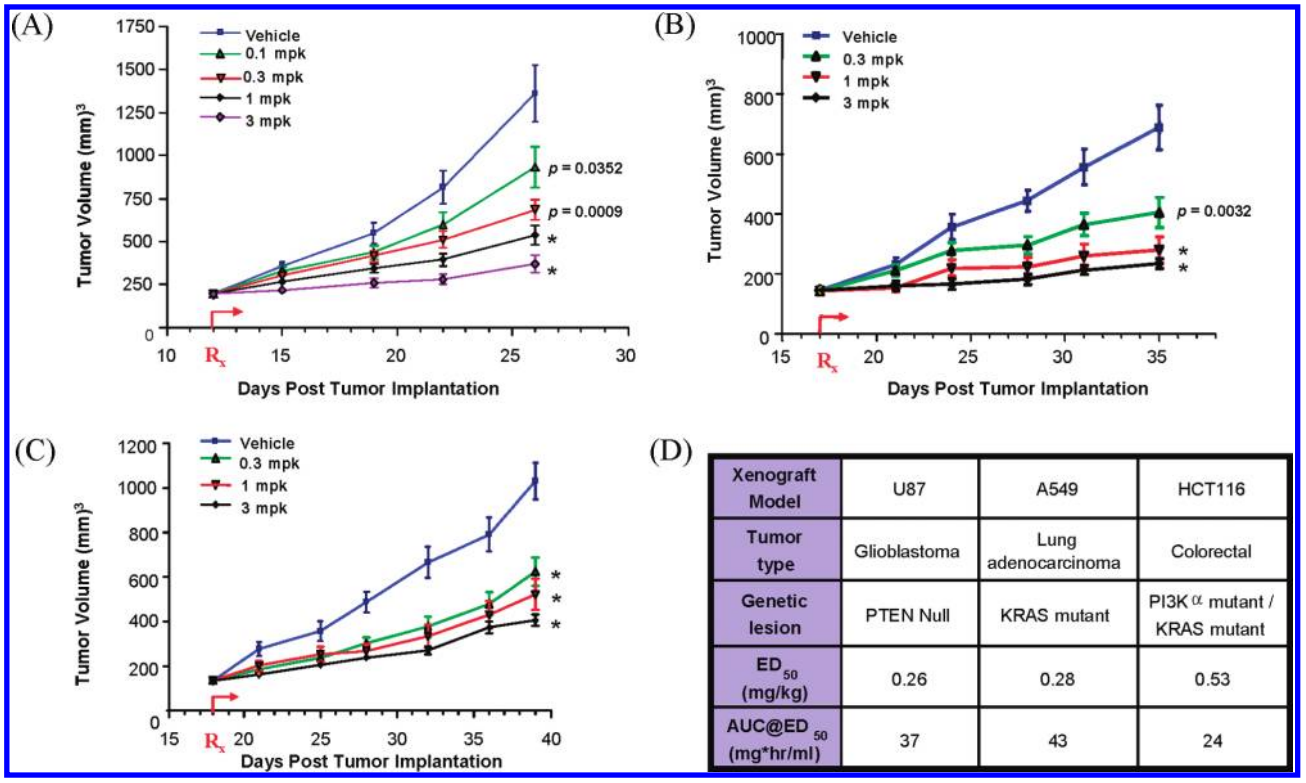

Xenograft Model	U87	A549	HCT116
Tumor type	Glioblastoma	Lung adenocarcinoma	Colorectal
Genetic lesion	PTEN Null	KRAS mutant	PI3K$^{\alpha}$ mutant / KRAS mutant
ED_{50} (mg/kg)	0.26	0.28	0.53
AUC@ED_{50} (mg*hr/ml)	37	43	24

Figure 4. Daily dosing with **82** induced tumor stasis and growth delay in established xenograft models (A) U-87 MG glioblastoma, (B) A549 lung adenocarcinoma, and (C) HCT116 colon adenocarcinoma. Arrow denotes the first day of dosing. The 10 mpk arm had to be stopped on day 32 in the HCT116 model because of a drop in body weight to 85% of the initial body weight. (D) Summary of ED_{50} and AUC (at ED_{50}) values for the three studies. Asterisk denotes $p < 0.0001$ compared with the vehicle group.

***N*-(6-(2-(4-Methylphenylthio)pyrimidin-4-yl)benzo[*d*]thiazol-2-yl)acetamide (19).** Using 4-methylthiophenol and following the procedure used to prepare **6** gave **19** in 40% yield. MS (ESI pos ion) m/z: 393 ($M + H^+$). ^{1}H NMR (400 MHz, DMSO-d_6, δ): 12.52 (s, 1H), 8.65 (s, 1H), 8.62 (d, J = 5.02 Hz, 1H), 8.11 (d, J = 8.53 Hz, 1H), 7.84−7.78 (m, 2H), 7.55 (d, J = 7.53 Hz, 2H), 7.34 (d, J = 8.03 Hz, 2H), 2.41 (s, 3H), 2.23 (s, 3H).

***N*-(6-(2-(2-Methoxyphenylthio)pyrimidin-4-yl)benzo[*d*]thiazol-2-yl)acetamide (20).** Using 2-methoxythiophenol and following the procedure used to prepare **6** gave **20** in 46% yield. MS (ESI pos ion) m/z: 409 ($M + H^+$). ^{1}H NMR (400 MHz, DMSO-d_6, δ): 12.52 (s, 1H), 8.62 (s, 1H), 8.59 (d, J = 5.52 Hz, 1H), 8.07 (d, J = 8.53 Hz, 1H), 7.81−7.76 (m, 2H), 7.61 (d, J = 7.53 Hz, 1H), 7.55 (t, J = 7.78 Hz, 1H), 7.20 (d, J = 8.03 Hz, 1H), 7.07 (t, J = 7.53 Hz, 1H), 3.75 (s, 3H), 2.23 (s, 3H).

***N*-(6-(2-(3-Methoxyphenylthio)pyrimidin-4-yl)benzo[*d*]thiazol-2-yl)acetamide (21).** Using 3-methoxythiophenol and following the procedure used to prepare **6** gave **21** in 34% yield. MS (ESI pos ion) m/z: 409 ($M + H^+$). ^{1}H NMR (400 MHz, DMSO-d_6, δ): 12.41 (br s, 1H), 8.64−8.58 (m, 2H), 8.10 (d, J = 8.03 Hz, 1H), 7.83 (d, J = 5.02 Hz, 1H), 7.76 (d, J = 8.53 Hz, 1H), 7.44 (t, J = 8.03 Hz, 1H), 7.29−7.22 (m, 2H), 7.10 (d, J = 7.53 Hz, 1H), 3.81 (s, 3H), 2.20 (s, 3H).

***N*-(6-(2-(4-Methoxyphenylthio)pyrimidin-4-yl)benzo[*d*]thiazol-2-yl)acetamide (22).** Using 3-methoxythiophenol and following the procedure used to prepare **6** gave **22** in 38% yield. MS (ESI pos ion) m/z: 409 ($M + H^+$). ^{1}H NMR (400 MHz, DMSO-d_6, δ): 12.52 (s, 1H), 8.65 (s, 1H), 8.61 (d, J = 5.52 Hz, 1H), 8.11 (d, J = 8.53 Hz, 1H), 7.83−7.78 (m, 2H), 7.58 (d, J = 8.53 Hz, 2H), 7.09 (d, J = 8.53 Hz, 2H), 3.85 (s, 3H), 2.23 (s, 3H).

***N*-(6-(2-(3-Methylbenzyloxy)pyrimidin-4-yl)benzo[*d*]thiazol-2-yl)acetamide (24).** Using (3-methylphenyl)methanol and following the procedure used to prepare **6** gave **24** in 47% yield. This compound was purified by washing with Et_2O instead of by HPLC. MS (ESI pos ion) m/z: 391 ($M + H^+$). ^{1}H NMR (400 MHz, DMSO-d_6, δ): 12.55 (br s, 1H), 8.82 (s, 1H), 8.65 (d, J = 5.52 Hz, 1H), 8.24 (d, J = 8.53 Hz, 1H), 7.79 (d, J = 8.53 Hz, 1H), 7.76 (d, J = 5.02 Hz, 1H), 7.35 (s, 1H), 7.33−7.25 (m, 2H), 7.15 (d, J = 6.02 Hz, 1H), 5.47 (s, 2H), 2.33 (s, 3H), 2.20 (s, 3H).

***N*-(6-(2-(3-Methoxybenzyloxy)pyrimidin-4-yl)benzo[*d*]thiazol-2-yl)acetamide (25).** Using (3-methoxyphenyl)methanol and following the procedure used to prepare **6** gave **25** in 69% yield. This compound was purified by washing with Et_2O instead of by HPLC. MS (ESI pos ion) m/z: 407 ($M + H^+$). ^{1}H NMR (400 MHz, DMSO-d_6, δ): 12.45 (br s, 1H), 8.77 (br s, 1H), 8.63 (d, J = 5.02 Hz, 1H), 8.21 (d, J = 8.03 Hz, 1H), 7.77−7.69 (m, 2H), 7.31 (t, J = 7.78 Hz, 1H), 7.11−7.06 (m, 2H), 6.90 (d, J = 9.54 Hz, 1H), 5.48 (s, 2H), 3.76 (s, 3H), 2.16 (s, 3H).

***N*-(6-(2-(4-Fluorobenzyloxy)pyrimidin-4-yl)benzo[*d*]thiazol-2-yl)acetamide (26).** Using (4-fluorophenyl)methanol and following the procedure used to prepare **6** gave **26** in 37% yield. This compound was purified by washing with Et_2O, MeOH, and Et_2O instead of by HPLC. MS (ESI pos ion) m/z: 395 ($M + H^+$). ^{1}H NMR (400 MHz, DMSO-d_6, δ): 12.51 (s, 1H), 8.88 (s, 1H), 8.68 (d, J = 5.02 Hz, 1H), 8.28 (d, J = 8.53 Hz, 1H), 7.85 (d, J = 8.53 Hz, 1H), 7.78 (d, J = 5.02 Hz, 1H), 7.58 (dd, J = 7.78, 5.77 Hz, 2H), 7.23 (t, J = 8.78 Hz, 2H), 5.50 (s, 2H), 2.23 (s, 3H).

***N*-(6-(2-(4-Methylbenzyloxy)pyrimidin-4-yl)benzo[*d*]thiazol-2-yl)acetamide (27).** Using (4-methylphenyl)methanol and following the procedure used to prepare **6** gave **27** in 54% yield. This compound was purified by washing with Et_2O instead of by HPLC. MS (ESI pos ion) m/z: 391 ($M + H^+$). ^{1}H NMR (400 MHz, DMSO-d_6, δ): 12.50 (br s, 1H), 8.81 (br s, 1H), 8.64 (d, J = 5.02 Hz, 1H), 8.24 (d, J = 9.03 Hz, 1H), 7.83−7.73 (m, 2H), 7.41 (d, J = 8.03 Hz, 2H), 7.21 (d, J = 7.53 Hz, 2H), 5.46 (s, 2H), 2.31 (s, 3H), 2.19 (s, 3H).

dx.doi.org/10.1021/jm1014605 |*J. Med. Chem.* 2011, 54, 1789–1811

***N*-(6-(2-(4-Methoxybenzyloxy)pyrimidin-4-yl)benzo[*d*]thiazol-2-yl)acetamide (28).** Using (4-methoxyphenyl)methanol and following the procedure used to prepare **6** gave **28** in 31% yield. This compound was purified by washing with Et_2O, MeOH, and Et_2O instead of by HPLC. MS (ESI pos ion) *m/z*: 407 ($M + H^+$). ^1H NMR (400 MHz, DMSO-d_6, δ): 12.50 (br s, 1H), 8.77 (br s, 1H), 8.63 (d, *J* = 5.02 Hz, 1H), 8.22 (d, *J* = 8.53 Hz, 1H), 7.73 (d, *J* = 5.02 Hz, 2H), 7.46 (d, *J* = 8.03 Hz, 2H), 6.96 (d, *J* = 8.53 Hz, 2H), 5.43 (s, 2H), 3.76 (s, 3H), 2.16 (s, 3H).

***N*-(6-(2-(Pyridin-4-ylmethoxy)pyrimidin-4-yl)benzo[*d*]thiazol-2-yl)acetamide (29).** Using 4-(hydroxymethyl)pyridine and following the procedure used to prepare **6** gave **29** in 51% yield. This compound was purified by washing with Et_2O instead of by HPLC. MS (ESI pos ion) *m/z*: 378 ($M + H^+$). ^1H NMR (400 MHz, DMSO-d_6, δ): 8.81 (s, 1H) 8.67 (d, *J* = 5.02 Hz, 1H), 8.59 (d, *J* = 5.52 Hz, 2H), 8.23 (d, *J* = 8.53 Hz, 1H), 7.81−7.76 (m, 2H), 7.49 (d, *J* = 5.52 Hz, 2H), 5.57 (s, 2H), 2.20 (s, 3H).

***N*-(6-(2-(3-(Pyridin-4-yl)propoxy)pyrimidin-4-yl)benzo[*d*]thiazol-2-yl)acetamide (30).** Using 3-(pyridin-4-yl)propan-1-ol and following the procedure used to prepare **6** gave **30** in 18% yield. This compound was purified by washing with Et_2O instead of by HPLC. MS (ESI pos ion) *m/z*: 406 ($M + H^+$). ^1H NMR (400 MHz, DMSO-d_6, δ): 12.48 (br s, 1H), 8.83 (s, 1H), 8.64 (d, *J* = 5.52 Hz, 1H), 8.47 (d, *J* = 5.52 Hz, 2H), 8.24 (d, *J* = 8.53 Hz, 1H), 7.84 (d, *J* = 8.53 Hz, 1H), 7.74 (d, *J* = 5.02 Hz, 1H), 7.30 (d, *J* = 5.52 Hz, 2H), 4.43 (t, *J* = 6.53 Hz, 2H), 2.80 (t, *J* = 7.78 Hz, 2H), 2.23 (s, 3H), 2.16−2.08 (m, 2H).

***N*-(6-(2-(4-Methoxyphenylsulfonamido)pyrimidin-4-yl)benzo[*d*]thiazol-2-yl)acetamide (37).** Using 4-methoxybenzenesulfonamide and DMSO and following the procedure used to prepare **6** gave **37** in 29% yield. The reaction was run at 125 °C overnight, and following HPLC purification, the material was washed with Et_2O, MeOH, and Et_2O to afford the product. MS (ESI pos ion) *m/z*: 456 ($M + H^+$). ^1H NMR (400 MHz, DMSO-d_6, δ): 12.53 (s, 1H), 11.66 (br s, 1H), 8.59−8.52 (m, 2H), 8.15 (d, *J* = 8.53 Hz, 1H), 7.98 (d, *J* = 8.53 Hz, 2H), 7.85 (d, *J* = 8.53 Hz, 1H), 7.65 (d, *J* = 4.52 Hz, 1H), 7.10 (d, *J* = 9.03 Hz, 2H), 3.81 (s, 3H), 2.24 (s, 3H).

***N*-(6-(2-(4-Methoxy-*N*-methylphenylsulfonamido)pyrimidin-4-yl)benzo[*d*]thiazol-2-yl)acetamide (38).** Using 4-methoxy-*N*-methylbenzenesulfonamide and DMSO and following the procedure used to prepare **6** gave **38** in 25% yield. The reaction was run at 125 °C overnight. MS (ESI pos ion) *m/z*: 470 ($M + H^+$). ^1H NMR (400 MHz, DMSO-d_6, δ): 12.52 (br s, 1H), 8.64 (d, *J* = 5.02 Hz, 1H), 8.56 (s, 1H), 8.14 (d, *J* = 8.53 Hz, 1H), 7.99 (d, *J* = 8.53 Hz, 2H), 7.84 (d, *J* = 8.53 Hz, 1H), 7.71 (d, *J* = 5.02 Hz, 1H), 7.10 (d, *J* = 9.03 Hz, 2H), 3.82 (s, 3H), 3.69 (s, 3H), 2.23 (s, 3H).

***N*-(6-(2-(*N*-Ethyl-4-methoxyphenylsulfonamido)pyrimidin-4-yl)benzo[*d*]thiazol-2-yl)acetamide (39).** Using 4-methoxy-*N*-ethylbenzenesulfonamide and DMSO and following the procedure used to prepare **6** gave **39** in 12% yield. The reaction was run at 125 °C overnight. MS (ESI pos ion) *m/z*: 484 ($M + H^+$). ^1H NMR (400 MHz, DMSO-d_6, δ): 12.51 (br s, 1H), 8.63 (d, *J* = 5.02 Hz, 1H), 8.48 (s, 1H), 8.08 (d, *J* = 8.53 Hz, 1H), 7.98 (d, *J* = 8.53 Hz, 2H), 7.83 (d, *J* = 8.53 Hz, 1H), 7.68 (d, *J* = 5.02 Hz, 1H), 7.10 (d, *J* = 8.53 Hz, 2H), 4.37−4.26 (m, 2H), 3.82 (s, 3H), 2.23 (s, 3H), 1.42 (t, *J* = 6.53 Hz, 3H).

Procedure for the Synthesis of 9, 11, 23, 31−35, 40, and 42−44. *N*-(6-(2-(Benzyloxy)pyrimidin-4-yl)benzo[*d*]thiazol-2-yl)acetamide (9). Compound **5** (60.8 mg, 0.200 mmol) and benzyl alcohol (0.20 mL, 1.9 mmol) were suspended in pyridine (0.84 mL) and sealed in a microwave vial. The vial was heated in the CEM microwave at 120 °C and 300 W with a 5 min ramp time and 20 min run time. The mixture was cooled to room temperature, concentrated, and purified on HPLC (10% → 95% MeCN/H_2O with 0.1% TFA over 28−40 min) to afford **9** (4.4 mg, 6% yield). MS (ESI pos ion) *m/z*: 377 ($M + H^+$). ^1H NMR (400 MHz, DMSO-d_6, δ): 12.51 (br s, 1H), 8.87 (s, 1H), 8.67 (s, 1H), 8.27 (d, *J* = 6.53 Hz, 1H), 7.84 (d, *J* = 7.03 Hz, 1H), 7.77 (s, 1H), 7.60−7.29 (m, 5H), 5.51 (s, 2H), 2.23 (s, 3H).

***N*-(6-(2-(Benzylamino)pyrimidin-4-yl)benzo[*d*]thiazol-2-yl)acetamide (11).** Using benzylamine and following the procedure used to prepare **9** gave **11** in 22% yield. MS (ESI pos ion) *m/z*: 376 ($M + H^+$). ^1H NMR (400 MHz, DMSO-d_6, δ): 12.48 (s, 1H), 8.73 (s, 1H), 8.36 (d, *J* = 5.52 Hz, 1H), 8.19 (d, *J* = 8.53 Hz, 1H), 7.93 (br s, 1H), 7.81 (d, *J* = 9.03 Hz, 1H), 7.44−7.36 (m, 2H), 7.32 (d, *J* = 14.56 Hz, 2H), 7.29−7.18 (m, 2H), 4.63 (br s, 2H), 2.23 (s, 3H).

***N*-(6-(2-(3-Fluorobenzyloxy)pyrimidin-4-yl)benzo[*d*]thiazol-2-yl)acetamide (23).** Using (3-fluorophenyl)methanol and following the procedure used to prepare **9** gave **23** in 22% yield. The mixture was reheated a second time in the microwave at 120 °C and 300 W with a 5 min ramp time and 10 min run time. MS (ESI pos ion) *m/z*: 395 ($M + H^+$). ^1H NMR (400 MHz, DMSO-d_6, δ): 12.51 (br s, 1H), 8.87 (s, 1H), 8.68 (d, *J* = 3.51 Hz, 1H), 8.27 (d, *J* = 8.03 Hz, 1H), 7.84 (d, *J* = 8.03 Hz, 1H), 7.78 (d, *J* = 3.51 Hz, 1H), 7.52−7.29 (m, 3H), 7.22−7.11 (m, 1H), 5.53 (s, 2H), 2.23 (s, 3H).

***N*-(6-(2-(3-(Pyridin-3-yl)propoxy)pyrimidin-4-yl)benzo[*d*]thiazol-2-yl)acetamide (31).** Using 3-pyridinepropanol and following the procedure used to prepare **9** gave **31** in 18% yield. MS (ESI pos ion) *m/z*: 406 ($M + H^+$). ^1H NMR (400 MHz, DMSO-d_6, δ): 12.51 (s, 1H), 8.86−8.80 (m, 2H), 8.72 (d, *J* = 5.02 Hz, 1H), 8.64 (d, *J* = 5.52 Hz, 1H), 8.39 (d, *J* = 8.03 Hz, 1H), 8.25 (dd, *J* = 8.53, 1.51 Hz, 1H), 7.91−7.82 (m, 2H), 7.75 (d, *J* = 5.02 Hz, 1H), 4.47 (t, *J* = 6.27 Hz, 2H), 2.98 (t, *J* = 7.53 Hz, 2H), 2.23 (s, 3H), 2.22−2.14 (m, 2H).

***N*-(6-(2-(3-Phenylpropoxy)pyrimidin-4-yl)benzo[*d*]thiazol-2-yl)acetamide (32).** Using 3-phenylpropan-1-ol and following the procedure used to prepare **9** gave **32** in 6% yield. MS (ESI pos ion) *m/z*: 405 ($M + H^+$). ^1H NMR (400 MHz, DMSO-d_6, δ): 12.50 (s, 1H), 8.83 (s, 1H), 8.64 (d, *J* = 5.02 Hz, 1H), 8.25 (d, *J* = 8.53 Hz, 1H), 7.84 (d, *J* = 8.53 Hz, 1H), 7.74 (d, *J* = 5.52 Hz, 1H), 7.34−7.24 (m, 4H), 7.23−7.16 (m, 1H), 4.42 (t, *J* = 6.53 Hz, 2H), 2.78 (t, *J* = 7.53 Hz, 2H), 2.23 (s, 3H), 2.14−2.04 (m, 2H).

***N*-(6-(2-(3-Morpholinopropoxy)pyrimidin-4-yl)benzo[*d*]thiazol-2-yl)acetamide (33).** Using 4-(3-hydroxypropyl)morpholine and following the procedure used to prepare **9** gave **33** in 5% yield as a TFA salt. Before HPLC purification, the crude material was filtered through silica gel (15:1 DCM/MeOH → 5:1 DCM/2 N ammonia in MeOH). MS (ESI pos ion) *m/z*: 414 ($M + H^+$). ^1H NMR (400 MHz, DMSO-d_6, δ): 12.52 (br s, 1H), 9.83 (br s, 1H), 8.85 (s, 1H), 8.67 (d, *J* = 5.52 Hz, 1H), 8.27 (d, *J* = 8.03 Hz, 1H), 7.86 (d, *J* = 8.53 Hz, 1H), 7.78 (d, *J* = 5.02 Hz, 1H), 4.51 (t, *J* = 5.77 Hz, 2H), 4.05−3.95 (m, 2H), 3.71−3.61 (m, 2H), 3.51 (d, *J* = 11.04 Hz, 2H), 3.40−3.29 (m, 2H), 3.16−3.05 (m, 2H), 2.30−2.16 (m, 5H).

***N*-(6-(2-(2-Morpholinoethoxy)pyrimidin-4-yl)benzo[*d*]thiazol-2-yl)acetamide (34).** Using 4-(2-hydroxyethyl)morpholine and following the procedure used to prepare **9** gave **34** in 5% yield as a TFA salt. MS (ESI pos ion) *m/z*: 400 ($M + H^+$). ^1H NMR (400 MHz, DMSO-d_6, δ): 12.53 (br s, 1H), 9.74 (br s, 1H), 8.87 (s, 1H), 8.71 (d, *J* = 5.52 Hz, 1H), 8.29 (d, *J* = 8.53 Hz, 1H), 7.89−7.82 (m, 2H), 4.80 (br s, 2H), 3.99−3.89 (m, 2H), 3.76−3.71 (m, 2H), 3.69−3.64 (m, 2H), 3.23−3.18 (m, 2H), 2.24 (s, 3H). (The additional two methylene protons could be buried under the H_2O peak, which ranges from 3.64−3.35.)

***N*-(6-(2-(3-Methoxypropoxy)pyrimidin-4-yl)benzo[*d*]thiazol-2-yl)acetamide (35).** Using 3-methoxypropan-1-ol and following the procedure used to prepare **9** gave **35** in 7% yield. MS (ESI pos ion) *m/z*: 359 ($M + H^+$). ^1H NMR (400 MHz, DMSO-d_6, δ): 12.50 (s, 1H), 8.85 (s, 1H), 8.64 (d, *J* = 5.02 Hz, 1H), 8.27 (d, *J* = 9.03 Hz, 1H), 7.85 (d, *J* = 8.53 Hz, 1H), 7.74 (d, *J* = 5.02 Hz, 1H), 4.46 (t, *J* = 6.27 Hz, 2H), 3.51 (t, *J* = 6.27 Hz, 2H), 3.27 (s, 3H), 2.23 (s, 3H), 2.02 (quin, *J* = 6.40 Hz, 2H).

***N*-(6-(2-(2-Fluorophenylsulfonamido)pyrimidin-4-yl)benzo[*d*]thiazol-2-yl)acetamide (40).** Using 2-fluorobenzenesulfonamide

and following the procedure used to prepare **9** gave **40** in 17% yield. Before HPLC purification, the crude material was filtered through silica gel (10:1 DCM/MeOH). After HPLC purification, the material was washed with Et_2O to afford **40**. MS (ESI pos ion) *m/z*: 444 ($M + H^+$). ^1H NMR (400 MHz, DMSO-d_6, δ): 12.54 (br s, 1H), 8.57−8.43 (m, 2H), 8.18 (t, *J* = 8.28 Hz, 1H), 7.99 (d, *J* = 7.53 Hz, 1H), 7.80 (d, *J* = 8.53 Hz, 1H), 7.72−7.57 (m, 2H), 7.49−7.42 (m, 1H), 7.37 (t, *J* = 9.03 Hz, 1H), 2.24 (s, 3H).

***N*-(6-(2-(3-Fluorophenylsulfonamido)pyrimidin-4-yl)benzo[*d*]thiazol-2-yl)acetamide (42).** Using 3-fluorobenzenesulfonamide and following the procedure used to prepare **9** gave **42** in 6% yield. Before HPLC purification, the crude material was filtered through silica gel (10:1 DCM/MeOH). MS (ESI pos ion) *m/z*: 444 ($M + H^+$). ^1H NMR (400 MHz, DMSO-d_6, δ): 12.54 (s, 1H), 8.59−8.53 (m, 2H), 8.10 (d, *J* = 9.03 Hz, 1H), 7.88−7.80 (m, 3H), 7.69−7.61 (m, 2H), 7.53−7.45 (m, 1H), 2.24 (s, 3H).

***N*-(6-(2-(4-Fluorophenylsulfonamido)pyrimidin-4-yl)benzo[*d*]thiazol-2-yl)acetamide (43).** Using 4-fluorobenzenesulfonamide and following the procedure used to prepare **9** gave **43** in 7% yield. Before HPLC purification, the crude material was filtered through silica gel (10:1 DCM/MeOH). MS (ESI pos ion) *m/z*: 444 ($M + H^+$). ^1H NMR (400 MHz, DMSO-d_6, δ): 12.54 (s, 1H), 8.58 (s, 1H), 8.55 (d, *J* = 5.02 Hz, 1H), 8.14−8.07 (m, 3H), 7.85 (d, *J* = 8.53 Hz, 1H), 7.66 (d, *J* = 6.02 Hz, 1H), 7.43 (t, *J* = 8.78 Hz, 2H), 2.24 (s, 3H).

***N*-(6-(2-(4-Methylphenylsulfonamido)pyrimidin-4-yl)benzo[*d*]thiazol-2-yl)acetamide (44).** Using 4-methylbenzenesulfonamide and following the procedure used to prepare **9** gave **44** in 13% yield. Instead of HPLC purification, the crude material was filtered through silica gel (10:1 DCM/MeOH). This filtrate was concentrated, treated with Et_2O, and filtered. The solid was washed with Et_2O, MeOH, and Et_2O to afford **44**. MS (ESI pos ion) *m/z*: 440 ($M + H^+$). ^1H NMR (400 MHz, DMSO-d_6, δ): 12.53 (s, 1H), 11.77 (br s, 1H), 8.55 (d, *J* = 4.52 Hz, 1H), 8.52 (br s, 1H), 8.13 (d, *J* = 7.53 Hz, 1H), 7.93 (d, *J* = 8.03 Hz, 2H), 7.84 (d, *J* = 8.53 Hz, 1H), 7.66−7.60 (m, 1H), 7.39 (d, *J* = 8.03 Hz, 2H), 2.35 (s, 3H), 2.24 (s, 3H).

***N*-(6-(2-Benzylpyrimidin-4-yl)benzo[*d*]thiazol-2-yl)acetamide (12).** *N*-(6-(2-Chloropyrimidin-4-yl)benzo[*d*]thiazol-2-yl)acetamide (**5**, 59.0 mg, 0.194 mmol) was suspended in THF (1.8 mL) to which $Pd(PPh_3)_4$ (25.6 mg, 0.022 mmol) and benzylzinc bromide (0.5 M solution in THF, 0.55 mL, 0.275 mmol) were added under argon. The reaction solution was stirred at room temperature. After 2 h, the mixture was heated to 80 °C, and stirring was continued under argon. After 100 min, additional $Pd(PPh_3)_4$ (21 mg, 0.018 mmol) and benzylzinc bromide (0.5 M solution in THF, 0.57 mL, 0.285 mmol) were added, and the mixture was stirred. After another hour, additional benzylzinc bromide (0.5 M solution in THF, 0.73 mL, 0.365 mmol) was added, and stirring was continued at 80 °C. The mixture was stirred overnight and quenched with saturated ammonium chloride (1.5 mL) and 0.5 M EDTA (2.5 mL), extracted with 10:1 DCM/MeOH, and the organic phases were dried over Na_2SO_4, filtered through Celite, and concentrated. The crude concentrate was purified on a silica gel column (20:1 → 5:1 DCM/MeOH), and the product-containing fractions were collected, concentrated, treated with Et_2O and MeOH, and filtered. The solid was collected and purified on HPLC (10% 95% MeCN/H_2O with 0.1% TFA over 40 min) to provide **12** (8 mg, 11% yield). MS (ESI pos ion) *m/z*: 361 ($M + H^+$). ^1H NMR (400 MHz, DMSO-d_6, δ): 12.50 (s, 1H), 8.85 (s, 1H), 8.78 (d, *J* = 5.5 Hz, 1H), 8.29 (d, *J* = 8.0 Hz, 1H), 7.95 (d, *J* = 5.5 Hz, 1H), 7.85 (d, *J* = 8.5 Hz, 1H), 7.38 (m, 2H), 7.31 (m, 2H), 7.21 (m, 1H), 4.28 (s, 2H), 2.23 (s, 3H).

***N*-(6-(2-Phenethylpyrimidin-4-yl)benzo[*d*]thiazol-2-yl)acetamide (13).** Compound **5** (277 mg, 0.909 mmol) and $Pd(PPh_3)_4$ (160 mg, 0.138 mmol) were suspended in THF (5.0 mL), and phenethylzinc(II) bromide (0.5 M in THF, 8.3 mL, 4.2 mmol) was added. The flask was fitted with a reflux condenser and was put in a preheated oil bath (80 °C) and stirred for 1 h. The mixture was cooled to room temperature and was treated with saturated ammonium chloride (5 mL) and 0.5 M aqueous EDTA (8 mL). The mixture was stirred at room temperature for 5 min and then was filtered through a Celite pad, which was washed with H_2O, MeOH, DCM, and EtOAc. The layers of the filtrate were separated, and the aqueous phase was extracted with DCM. The organic phases were combined, dried over Na_2SO_4, filtered, concentrated, and purified on silica gel (30:1 → 20:1 DCM/MeOH). The fractions with product were collected, concentrated, treated with MeOH, and filtered. The solid was washed with MeOH, Et_2O, and MeOH. The filtrate and solid were combined, concentrated, treated with DCM, and filtered. The solid was washed with DCM and MeOH and was found to be less than 95% pure by HPLC. The filtrate and solid were combined, concentrated, and purified on HPLC (10% → 100% MeCN/H_2O with 0.1% TFA over 28 min) to afford **13** (26.7 mg, 8% yield). MS (ESI pos ion) *m/z*: 375 ($M + H^+$). ^1H NMR (400 MHz, $CDCl_3$, δ): 8.80 (d, *J* = 5.48 Hz, 1H), 8.64 (d, *J* = 1.37 Hz, 1H), 8.23 (dd, *J* = 8.61, 1.56 Hz, 1H), 7.91 (d, *J* = 8.80 Hz, 1H), 7.68 (d, *J* = 5.48 Hz, 1H), 7.34−7.19 (m, 5H), 3.37−3.53 (m, 2H), 3.19−3.34 (m, 2H), 2.46 (s, 3H).

***N*-(6-(2-(2-Phenylpropan-2-ylamino)pyrimidin-4-yl)benzo[*d*]thiazol-2-yl)acetamide (36).** A solution of **5** (0.100 g, 0.328 mmol), cumylamine (0.05 mL, 0.4 mmol), and Cs_2CO_3 (0.2 g, 0.6 mmol) in DMF (1 mL) was heated in the CEM microwave at 180 °C and 180 W for 20 min. The mixture was diluted with DCM, washed with H_2O three times, dried over Na_2SO_4, and concentrated. The residue was purified by HPLC (5% → 100% MeCN/H_2O with 0.05% TFA) to give **36** as an off-white solid (2.5 mg, 2% yield). MS (ESI pos ion) *m/z*: 404 ($M + H^+$). ^1H NMR (300 MHz, $CDCl_3$, δ): 10.40 (br s, 1H), 8.85 (d, *J* = 4.82 Hz, 1H), 8.05 (d, *J* = 6.43 Hz, 1H), 7.78 (dd, *J* = 7.82, 6.36 Hz, 1H), 7.73−7.70 (m, 2H), 7.57−7.52 (m, 2H), 7.43 (t, *J* = 7.67 Hz, 2H), 7.32−7.26 (m, 1H), 7.08 (d, *J* = 6.58 Hz, 1H), 2.42 (s, 3H), 1.88 (s, 6H).

Procedure for the Synthesis of 41 and 45. *N*-(6-(2-(2-Fluoro-*N*-methylphenylsulfonamido)pyrimidin-4-yl)benzo[*d*]thiazol-2-yl)acetamide (41). A microwave vial equipped with a stir bar was charged with 2-fluoro-*N*-methylbenzenesulfonamide (0.23 g, 1.2 mmol) in DMF (3 mL). Then NaH (0.12 g, 4.9 mmol) was added to the mixture and the mixture was allowed to stir for 30 min. Then $Pd(OAc)_2$ (11 mg, 0.049 mmol), **5** (150 mg, 0.492 mmol), and Xantphos (10 mg, 0.017 mmol) were added to the mixture. The vial was capped and placed into a CEM microwave for 10 min at 100 °C, while 100 W of energy was supplied via Powermax. The mixture was added to a round-bottomed flask and diluted with H_2O (150 mL). The mixture was allowed to stir overnight. The resulting precipitate was collected by filtration and washed with hexanes (3 × 50 mL) and 1:1 hexanes/Et_2O (50 mL). Then the crude material was recrystallized from 1:1 MeOH/DCM and then from hexanes to give **41** (35 mg, 16% yield) as a brown solid. MS (ESI pos ion) *m/z*: 458 ($M + H^+$). ^1H NMR (400 MHz, DMSO-d_6, δ): 12.50 (s, 1H), 8.64 (d, *J* = 5.02 Hz, 1H), 8.48 (s, 1H), 8.22 (t, *J* = 7.53 Hz, 1H), 7.99 (d, *J* = 8.53 Hz, 1H), 7.79 (d, *J* = 8.53 Hz, 1H), 7.76−7.69 (m, 2H), 7.52−7.39 (m, 2H), 3.70 (s, 3H), 2.23 (s, 3H).

***N*-(6-(2-(4-Methyl-*N*-methylphenylsulfonamido)pyrimidin-4-yl)benzo[*d*]thiazol-2-yl)acetamide (45).** Using *N*-methyl-4-toluenesulfonamide and following the procedure used to prepare **41** gave **45** in 36% yield. MS (ESI pos ion) *m/z*: 454 ($M + H^+$). ^1H NMR (400 MHz, DMSO-d_6, δ): 12.52 (s, 1H), 8.64 (s, 1H), 8.48 (s, 1H), 8.10 (d, *J* = 5.0 Hz, 1H), 7.93 (s, 2H), 7.83 (s, 1H), 7.71 (s, 1H), 7.40 (s, 2H), 3.70 (s, 3H), 2.37 (s, 3H), 2.24 (s, 3H).

***N*-(4-Chloropyrimidin-2-yl)-4-methoxybenzamide (47).** A mixture of 4-chloropyrimidin-2-amine (**46**, 0.65 g, 5.0 mmol), triethylamine (1.4 mL, 10 mmol), and 4-anisoyl chloride (0.66 mL, 5.0 mmol) in DCM (20 mL) was stirred for 16 h at room temperature. Then the mixture was concentrated and the residue was purified on silica gel (0% → 8% MeOH in DCM) to afford **47** (70 mg, 5%) as a white solid. MS (ESI pos ion) *m/z*: 264 ($M + H^+$). ^1H NMR (300 MHz, $CDCl_3$, δ):

8.56 (s, 1H), 8.54 (s, 1H), 8.29 (d, J = 5.70 Hz, 1H), 7.91−7.86 (m, 2H), 7.04−7.00 (m, 2H), 3.91 (s, 3H).

***N*-(4-(2-Acetamidobenzo[d]thiazol-6-yl)pyrimidin-2-yl)-4-methoxybenzamide (48).** To a mixture of **47** (70 mg, 0.27 mmol), **4** (130 mg, 0.40 mmol), and $Pd(PPh_3)_4$ (31 mg, 0.027 mmol) under N_2 was added aqueous 2 M Na_2CO_3 (0.5 mL, 1 mmol) and 1,4-dioxane (3 mL). The flask was placed into a preheated (90 °C) bath, and the mixture was allowed to stir under an inert atmosphere overnight. The resulting mixture was concentrated and diluted with DMSO (2 mL) and purified by HPLC (5% → 95% MeCN in H_2O). The fractions with pure product were concentrated, diluted with DCM, and washed with aqueous Na_2CO_3 solution. The organic layer was dried over Na_2SO_4 and concentrated to give **48** (35 mg, 31%) as a white solid. MS (ESI pos ion) m/z: 420 ($M + H^+$). ^1H NMR (300 MHz, $CDCl_3$, δ): 10.95 (br s, 1H), 8.85 (s, 1H), 8.72 (d, J = 5.26 Hz, 1H), 8.61 (d, J = 1.61 Hz, 1H), 8.16 (dd, J = 8.62, 1.75 Hz, 1H), 7.99−7.92 (m, 2H), 7.84 (d, J = 8.48 Hz, 1H), 7.50 (d, J = 5.41 Hz, 1H), 7.00 (d, J = 8.92 Hz, 2H), 3.90 (s, 3H), 2.33 (s, 3H).

***N*-(6-(2-Chloropyridin-4-yl)benzo[*d*]thiazol-2-yl)acetamide (50).** 2-Chloro-4-iodopyridine (**49**, 500 mg, 2.09 mmol) was dissolved in 1,4-dioxane (15 mL). Then **4a** (0.8 g, 3 mmol), $Ph(PPh_3)_4$ (0.3 g, 0.3 mmol), and aqueous 2 M Na_2CO_3 (2 mL, 4 mmol) were added to the mixture. The flask was fitted with a reflux condenser, placed into a preheated (90 °C) bath, and stirred under inert atmosphere for 3 h. The mixture was allowed to cool to ambient temperature and was diluted with DCM and saturated $NaHCO_3$. The organic layer was collected by extracting with DCM (3 × 20 mL). The organics were combined, dried over Na_2SO_4, filtered, and concentrated. The residue was diluted with Et_2O (50 mL) and allowed to stir for 10 min. The precipitate was collected by filtration and washed with Et_2O to afford **50** (0.200 g, 32% yield) as a tan crystalline solid. MS (ESI pos ion) m/z: 304 ($M + H^+$). ^1H NMR (400 MHz, DMSO-d_6, δ): 12.49 (br s, 1H), 8.53 (s, 1H), 8.47 (d, J = 5.09 Hz, 1H), 7.94−7.89 (m, 2H), 7.86−7.79 (m, 2H), 2.22 (s, 3H).

***N*-(6-(2-(4-Methoxyphenylsulfonamido)pyridin-4-yl)benzo-[*d*]thiazol-2-yl)acetamide (51).** A microwave vial with a magnetic stir bar was charged with 4-methoxybenzenesulfonamide (0.25 g, 1.3 mmol) in DMF (3 mL). Sodium hydride (63 mg, 2.6 mmol) was added, and the mixture was allowed to stir for 15 min. Then **50** (160 mg, 0.528 mmol), $Pd(OAc)_2$ (12 mg, 0.053 mmol), and Xantphos (10 mg, 0.017 mmol) were added to the mixture. The vial was capped and placed into a CEM microwave for 20 min at 120 °C, while 100 W of energy was supplied via Powermax. The reaction mixture was then transferred to a round-bottomed flask and diluted with EtOAc (20 mL) while stirring. After 20 min, the mixture was filtered and the resulting precipitate was collected. The precipitate was diluted with DMSO and purified by HPLC to afford **51** (28 mg, 12% yield) as a tan crystalline solid. MS (ESI pos ion) m/z: 455 ($M + H^+$). ^1H NMR (400 MHz, DMSO-d_6, δ): 7.92 (d, J = 10.04 Hz, 2H), 7.85−7.68 (m, 3H), 7.65−7.54 (m, 2H), 7.46 (s, 1H), 6.96−6.84 (m, 3H), 6.70 (br s, 1H), 3.74 (s, 3H), 2.09 (s, 3H).

***N*-(5-Bromopyridin-3-yl)-4-methoxybenzenesulfonamide (53).** To a round-bottomed flask was added 5-bromopyridin-3-amine, **52** (400 mg, 2.31 mmol), EtOH (10 mL), and 4-methoxybenzene-1-sulfonyl chloride (0.96 g, 4.6 mmol). The resulting mixture was allowed to stir at ambient temperature overnight while under inert atmosphere. The mixture was diluted with DCM and saturated $NaHCO_3$ and extracted with DCM (3 × 25 mL). The organics were combined, dried over Na_2SO_4, filtered, concentrated, and purified by ISCO silica gel chromatography in a gradient of 10% → 30% EtOAc/DCM over 30 min to afford **53** (0.165 g, 21% yield) as a white crystalline solid. MS (ESI pos ion) m/z: 343 ($M + H^+$, ^{79}Br), 345 ($M + H^+$, ^{81}Br). ^1H NMR (400 MHz, DMSO-d_6, δ): 10.73 (s, 1H), 8.38 (s, 1H), 8.28 (s, 1H), 7.74 (d, J = 8.53 Hz, 2H), 7.67 (s, 1H), 7.11 (d, J = 8.53 Hz, 2H), 3.81 (s, 3H).

***N*-(6-(5-(4-Methoxyphenylsulfonamido)pyridin-3-yl)benzo-[*d*]thiazol-2-yl)acetamide (54).** To a microwave vial charged with **53** (165 mg, 0.481 mmol) in 1,4-dioxane (3 mL) was added **4a** (223 mg, 0.701 mmol), Fibercat (24 mg, 20% Pd), and aqueous 2 M Na_2CO_3 (0.6 mL, 1.2 mmol). A stir bar was added to the vial, and then the vial was capped and placed into CEM microwave for 10 min at 100 °C, while 100 W of energy was supplied via Powermax. The mixture was allowed to cool to ambient temperature and diluted with DCM and saturated $NaHCO_3$. The organic layer was collected by extracting with DCM (3 × 20 mL). The organic extracts were combined, dried over Na_2SO_4, filtered, and concentrated. The mixture was allowed to stand for 2 h, and the precipitate was collected by filtration. The solid was washed with 1:1 EtOAc/Et_2O and then with Et_2O to afford **54** (35 mg, 16% yield) as a tan solid. MS (ESI pos ion) m/z: 455 ($M + H^+$). ^1H NMR (400 MHz, DMSO-d_6, δ): 12.42 (s, 1H), 8.59 (s, 1H), 8.24 (s, 2H), 7.86−7.70 (m, 4H), 7.63 (s, 1H), 7.08 (d, J = 5.52 Hz, 2H), 3.79 (s, 3H), 2.22 (s, 3H).

***N*-(6-(6-Chloropyrazin-2-yl)benzo[*d*]thiazol-2-yl)acetamide (56).** 2,6-Dichloropyrazine (**55**, 1.119 g, 7.511 mmol), **4a** (3.07 g, 9.65 mmol), $Pd(dppf)_2Cl_2$/DCM complex (519.9 mg, 0.637 mmol), and K_2CO_3 (2.992 g, 21.65 mmol) were suspended in 1,2-dimethoxyethane (50 mL), and H_2O (15 mL) was added. The flask was fitted with a reflux condenser and placed in a preheated oil bath (90 °C) and stirred under N_2. After 1.5 h, the mixture was cooled to room temperature and filtered, and the solid was washed with 1,2-dimethoxyethane. The solid was set aside, and the filtrate was concentrated, treated with Et_2O, and filtered. The solid from this filtration was washed with Et_2O, H_2O, and three cycles of MeOH and Et_2O. The solid was collected and dried to afford **56** (1.954 g, 73% purity, 62% yield). For characterization purposes, a portion (∼100 mg) was purified on HPLC (10% → 95% MeCN/H_2O with 0.1% TFA over 30 min). The fractions with product were collected, concentrated, and washed with Et_2O, MeOH, and Et_2O. The solid was collected and dried under high vacuum in a H_2O bath (50 °C). MS (ESI pos ion) m/z: 305 ($M + H^+$). ^1H NMR (400 MHz, DMSO-d_6, δ): 12.50 (s, 1H), 9.32 (s, 1H), 8.77 (s, 1H), 8.72 (s, 1H), 8.20 (d, J = 8.53 Hz, 1H), 7.86 (d, J = 8.53 Hz, 1H), 2.23 (s, 3H).

***N*-(6-(6-(4-Methoxyphenylsulfonamido)pyrazin-2-yl)benzo-[*d*]thiazol-2-yl)acetamide (57).** 4-Methoxybenzenesulfonamide (185.6 mg, 0.9913 mmol) was dissolved in DMSO (2.0 mL), and NaH (60% in mineral oil, 54.6 mg, 1.37 mmol) was added. The mixture was stirred under N_2 at room temperature for 1 h, and then **56** (84.8 mg, 0.278 mmol) was added. The flask was put in a preheated oil bath (125 °C) and was stirred under N_2 for 22 h. The mixture was cooled to room temperature, treated with MeOH, and filtered. The filtrate was concentrated and purified on HPLC (10% → 95% MeCN/H_2O with 0.1% TFA over 40 min) to afford **57** (5.0 mg, 4% yield). MS (ESI pos ion) m/z: 456 ($M + H^+$). ^1H NMR (400 MHz, DMSO-d_6, δ): 12.51 (s, 1H), 11.54 (s, 1H), 8.87 (s, 1H), 8.47 (s, 1H), 8.22 (s, 1H), 8.05 (d, J = 8.53 Hz, 1H), 7.97 (d, J = 8.53 Hz, 2H), 7.85 (d, J = 8.53 Hz, 1H), 7.13 (d, J = 8.53 Hz, 2H), 3.81 (s, 3H), 2.23 (s, 3H).

***N*-(6-(3-Aminophenyl)benzo[*d*]thiazol-2-yl)acetamide (59).** A mixture of **4a** (319 mg, 1.00 mmol), 3-bromobenzenamine (**58**, 0.17 g, 1.0 mmol), $Pd(PPh_3)_4$ (1.2 g, 1.0 mmol) in dioxane (2 mL), and aqueous Na_2CO_3 solution (2.0 M, 1.0 mL, 2.0 mmol) was heated in the microwave at 130 W and 100 °C for 20 min. Then the mixture was diluted with DCM and H_2O. The organic layer was separated, dried over Na_2SO_4, and concentrated. The residue was recrystallized to give **59** (0.050 g, 18%) as a brown solid. MS (ESI pos ion) m/z: 284 ($M + H^+$).

***N*-(6-(3-(4-Methoxyphenylsulfonamido)phenyl)benzo[*d*]thiazol-2-yl)acetamide (60).** To a mixture of **59** (0.030 g, 0.11 mmol) and pyridine (0.03 g, 0.3 mmol) in DCM (2 g) was added 4-methoxybenzene-1-sulfonyl chloride (0.05 g, 0.2 mmol) at room temperature. The mixture was stirred for 4 h, and then pyrrolidine (0.02 g, 0.3 mmol) was added. The resulting mixture was concentrated, diluted with DMSO (2 mL), and purified by HPLC (5% → 95% MeCN/H_2O). The fractions with pure product were collected, concentrated, diluted with DCM, and washed with aqueous Na_2CO_3 solution.

The organic layer was dried over Na_2SO_4 and concentrated to give **60** (0.035 g, 73%) as a white solid. MS (ESI pos ion) *m/z*: 454 ($M + H^+$). ^1H NMR (300 MHz, DMSO-d_6, δ): 12.39 (s, 1H), 10.26 (s, 1H), 8.12 (d, *J* = 1.61 Hz, 1H), 7.80 (d, *J* = 8.62 Hz, 1H), 7.75 (d, *J* = 8.92 Hz, 2H), 7.55 (dd, *J* = 8.55, 1.53 Hz, 1H), 7.41−7.31 (m, 3H), 7.10−7.04 (m, 3H), 3.79 (s, 3H), 2.22 (s, 3H).

***N*-(5-Bromo-2-cyanopyridin-3-yl)-4-methoxybenzenesulfonamide (62).** To a 100 mL round-bottomed flask was added 3-amino-5-bromopicolinonitrile **61** (0.7 g, 4 mmol) in 20 mL of THF. The solution was cooled to −40 °C and treated with LiHMDS (1.0 M in hexanes, 1 mL, 1 mmol) dropwise. The mixture was stirred for 10 min at the same temperature, and then 4-methoxybenzenesulfonyl chloride (0.9 g, 4 mmol) was added. The ice bath was removed, and the mixture was stirred at room temperature for 2 h. The mixture was then treated with brine and EtOAc, and the aqueous phase was extracted with EtOAc (2×). The combined organic phases were washed with brine, dried over $MgSO_4$, and concentrated. Purification by ISCO chromatography provided **62** (0.1 g, 8% yield) as a white solid. MS (ESI pos ion) *m/z*: 368 ($M + H^+$, ^{79}Br), 370 ($M + H^+$, ^{81}Br). ^1H NMR (400 MHz, $CDCl_3$, δ): 8.45 (d, *J* = 1.76 Hz, 1H), 8.30 (d, *J* = 1.76 Hz, 1H), 7.80 (d, *J* = 8.80 Hz, 2H), 7.06 (s, 1H), 7.00 (d, *J* = 8.80 Hz, 2H), 3.88 (s, 3H).

***N*-(6-(6-Cyano-5-(4-methoxyphenylsulfonamido)pyridin-3-yl)benzo[*d*]thiazol-2-yl)acetamide (63).** To a 100 mL round-bottomed flask were added **62** (100 mg, 0.272 mmol) and **4a** (108 mg, 0.339 mmol) in DME (10 mL). Argon was bubbled in for 2 min, and then aqueous Na_2CO_3 (2 M, 5 mL, 10 mmol) was added, followed by Pd(dppf)Cl_2 (80 mg, 0.11 mmol). The mixture was heated at 100 °C for 2 h and then was cooled to room temperature. The mixture was diluted with EtOAc (200 mL), causing precipitation. The suspension was filtered, and the filtrate was concentrated and purified via ISCO chromatographic purification (5% → 20% MeOH/DCM) to afford **63** (5 mg, 4% yield) as a brown solid. MS (ESI pos ion) *m/z*: 478 ($M - H$). ^1H NMR (400 MHz, DMSO-d_6, δ): 8.11 (d, *J* = 1.56 Hz, 1H), 8.05 (d, *J* = 1.96 Hz, 1H), 7.81 (d, *J* = 8.41 Hz, 1H), 7.78 (d, *J* = 1.96 Hz, 1H), 7.71 (d, *J* = 8.80 Hz, 2H), 7.48 (dd, *J* = 8.31, 1.66 Hz, 1H), 6.95 (d, *J* = 8.80 Hz, 2H), 3.75 (s, 3H), 2.22 (s, 3H).

5-Bromo-2-methylpyridin-3-amine (66). 5-Bromo-2-methyl-3-nitropyridine[40] (1.808 g, 8.331 mmol) was suspended in glacial acetic acid (16 mL) and H_2O (4 mL), and iron powder (1.411 g, 25.27 mmol) was added in portions over 5 min. The mixture was stirred under N_2 at room temperature for 70 min, using a water bath to cool the reaction flask. Then the mixture was diluted with EtOAc (20 mL) and the suspension was poured into 5 N NaOH (50 mL). The resulting emulsion was filtered through a pad of Celite, which was washed with H_2O and EtOAc. The layers were separated, and the aqueous phase was extracted with EtOAc (2 × 50 mL). The organic extracts and phases were combined, dried over Na_2SO_4, filtered, concentrated, and dried under high vacuum to afford **66** (1.86 g, 95% pure at 254 nm; 44% pure at 215 nm). Yield (based on purity at 215 nm): 52%. MS (ESI pos ion) *m/z*: 187 ($M + H^+$, ^{79}Br), 189 ($M + H^+$, ^{81}Br).

***N*-(6-(5-Amino-6-methylpyridin-3-yl)benzo[*d*]thiazol-2-yl) acetamide (67).** Compound **66** (224.9 mg, 1.202 mmol), compound **4a** (413.7 mg, 1.300 mmol), K_2CO_3 (549.4 mg, 3.975 mmol), and Pd(dppf)Cl_2/DCM complex (108.7 mg, 0.133 mmol) were suspended in DME (5.0 mL) and H_2O (1.25 mL). The flask was fitted with a reflux condenser, and argon was bubbled through for about 15 s. The flask was placed in a preheated oil bath (100 °C) and stirred under argon for 80 min. The mixture was cooled to room temperature, and the aqueous phase was removed via pipet. The mixture was then concentrated, treated with MeOH, and filtered. The solid was washed with MeOH, H_2O, MeOH, and Et_2O. The solid was collected and dried under high vacuum to afford **67** (179.7 mg, 50% yield). MS (ESI pos ion) *m/z*: 299 ($M + H^+$). ^1H NMR (400 MHz, DMSO-d_6, δ): 12.37 (br s, 1H), 8.18 (d, *J* = 1.00 Hz, 1H), 8.01 (d, *J* = 2.01 Hz, 1H), 7.79 (d, *J* = 8.53 Hz, 1H), 7.62 (dd, *J* = 8.28, 1.76 Hz, 1H), 7.21 (d, *J* = 1.51 Hz, 1H), 5.14 (s, 2H), 2.31 (s, 3H), 2.21 (s, 3H).

***N*-(6-(5-(4-Methoxyphenylsulfonamido)-6-methylpyridin-3-yl)benzo[*d*]thiazol-2-yl)acetamide (68).** Compound **67** (76.5 mg, 0.256 mmol), DMAP (31.4 mg, 0.257 mmol), and 4-methoxybenzene-1-sulfonyl chloride (224.7 mg, 1.087 mmol) were suspended in THF (1.5 mL) and pyridine (1.5 mL). The flask was fitted with reflux condenser and was placed in a preheated oil bath (65 °C) and stirred under N_2 for 90 min. More DMAP (33.2 mg, 0.272 mmol) and 4-methoxybenzene-1-sulfonyl chloride (163 mg, 0.789 mmol) were added, and stirring continued. After 4 h, more DMAP (20 mg) and 4-methoxybenzenesulfonyl chloride (85 mg, 0.41 mmol) were added. Stirring was continued for 30 min, and then the mixture was cooled to room temperature, concentrated, and purified on silica gel (20:1 → 10:1 DCM/MeOH). The fractions with product were collected, concentrated, treated with DCM, and filtered. The solid was washed with DCM and Et_2O, collected, and dried under high vacuum to afford **68** (64.0 mg, 53%). MS (ESI pos ion) *m/z*: 469 ($M + H^+$). ^1H NMR (400 MHz, DMSO-d_6, δ): 12.43 (s, 1H), 9.82 (s, 1H), 8.64 (d, *J* = 1.96 Hz, 1H), 8.18 (d, *J* = 1.56 Hz, 1H), 7.81 (d, *J* = 8.41 Hz, 1H), 7.63 (d, *J* = 6.65 Hz, 2H), 7.62−7.56 (m, 2H), 7.11 (d, *J* = 8.80 Hz, 2H), 3.83 (s, 3H), 2.22 (s, 3H), 2.19 (s, 3H).

***N*-(6-(6-Chloro-5-(4-methoxyphenylsulfonamido)pyridin-3-yl)benzo[*d*]thiazol-2-yl)acetamide (70).** A solution of 4-methoxybenzene-1-sulfonyl chloride (1 g, 5 mmol) and 3-amino-5-bromo-2-chloropyridine, **69** (0.45 g, 2.2 mmol), in pyridine (15 mL) was heated in a microwave vial at 100 °C for 20 min. The mixture was then concentrated and the residue was purified by silica gel column chromatography to afford the intermediate *N*-(5-bromo-2-chloropyridin-3-yl)-4-methoxybenzenesulfonamide (0.4 g, 49%).

Then *N*-(5-bromo-2-chloropyridin-3-yl)-4-methoxybenzenesulfonamide (0.15 g, 0.4 mmol), **4a** (0.18 g, 0.57 mmol), and Fibercat were mixed with 10% Na_2CO_3 (1 mL) and 1,4-dioxane (3 mL). The mixture was heated at 100 °C for 12 min. The mixture was filtered, and the filtrate was concentrated and washed with EtOAc. The collected solid was recrystallized in MeOH to afford **70** (0.08 g, 41% yield) as a white solid. MS (ESI pos ion) *m/z*: 489 ($M + H^+$). ^1H NMR (300 MHz, CD_3OD, δ): 8.44 (d, *J* = 2.34 Hz, 1H), 8.17 (d, *J* = 2.34 Hz, 1H), 8.11 (d, *J* = 1.61 Hz, 1H), 7.90−7.81 (m, 1H), 7.78−7.70 (m, 2H), 7.66 (dd, *J* = 8.48, 1.90 Hz, 1H), 7.07−6.97 (m, 2H), 3.85 (s, 3H), 2.29 (s, 3H). Anal. Calcd for ($C_{21}H_{17}ClN_4O_4S_2 \cdot 0.1DCM$) C, H, N.

Procedure for the Synthesis of 72, 73, 75, 78, and 80. *N*-(6-(6-Chloro-5-(2-chlorophenylsulfonamido)pyridin-3-yl) benzo[*d*]thiazol-2-yl)acetamide (75). In a 20 mL sealed tube, compound **69** (200 mg, 0.964 mmol) was dissolved in THF (2.0 mL). The solution was cooled to −78 °C, and LiHMDS (1.0 M in THF, 2.9 mL, 2.9 mmol) was added via syringe. The mixture was stirred at −78 °C for 10 min, and then 2-chlorobenzenesulfonyl chloride (203 mg, 0.964 mmol) was added. The dry ice bath was removed, and the mixture was allowed to warm to room temperature and was stirred for 17 h. Then the mixture was treated with ammonium chloride. To the mixture was added 2 N HCl to bring the aqueous phase to neutral pH. The mixture was extracted with ethyl acetate, and the organic phase was washed with H_2O and brine, dried over Na_2SO_4, filtered, and concentrated. The crude material was purified via ISCO silica gel chromatography (0−50% A/B, where A = DCM/MeOH (90:10) and B = DCM). This afforded the intermediate *N*-(5-bromo-2-chloropyridin-3-yl)-2-chlorobenzenesulfonamide (200 mg, 54% yield) as a tan solid.

In a 20 mL sealed tube, dioxane (0.500 mL) was added, the solvent was purged with N_2 for 5 min, and the tube was sealed. Then *N*-(5-bromo-2-chloropyridin-3-yl)-2-chlorobenzenesulfonamide (75 mg, 0.196 mmol), **4b** (64 mg, 0.22 mmol), and Na_2CO_3 (42 mg, 0.39 mmol) were added, and the flask was again purged with N_2 and sealed. Finally, Pd(dppf)Cl_2 (7.2 mg, 0.0098 mmol) was added, and the flask was

purged with N_2, sealed, and heated to 100 °C while the mixture was stirred for 1 h. The mixture was cooled to room temperature, concentrated, and extracted with DCM. A few drops of 2 N HCl were added, and the organic phase was washed with H_2O (2×), dried over Na_2SO_4, filtered, and concentrated. The crude material was purified via ISCO silica gel chromatography (0% → 100% A/B, where A = DCM/MeOH (90:10) and B = DCM) to afford **75** (23 mg, 93% purity, 24% yield) as a red solid. MS (ESI pos ion) *m/z*: 493 ($M + H^+$). ^{1}H NMR (400 MHz, DMSO-d_6, δ): 12.44 (s, 1H), 10.68 (br s, 1H), 8.62 (d, *J* = 2.15 Hz, 1H), 8.32 (d, *J* = 1.56 Hz, 1H), 8.02 (d, *J* = 2.35 Hz, 1H), 7.95 (dd, *J* = 7.92, 1.27 Hz, 1H), 7.83 (d, *J* = 8.41 Hz, 1H), 7.72−7.64 (m, 3H), 7.52−7.48 (m, 1H), 2.22 (s, 3H). Analytical HPLC: 94.5%.

***N*-(6-(6-Chloro-5-(2-(trifluoromethyl)phenylsulfonamido) pyridin-3-yl)benzo[*d*]thiazol-2-yl)acetamide (72).** Using 2-(trifluoromethyl)benzene-1-sulfonyl chloride and following the procedure used to prepare **75** gave **72** in 45% yield for the sulfonylation step and 62% yield for the Suzuki step. In addition, for the Suzuki coupling, microwave irradiation at 140 °C for 5 min was used. The final compound was purified by MPLC (Teledine ISCO Combiflash Companion). The crude residue was taken up in minimal DCM/MeOH and absorbed onto a minimal amount of silica gel, which was then packed into a 25 g custom loading cartridge and passed through a Redi-Sep prepacked silica gel column (80 g) using 99:1 DCM/MeOH → 95:5 DCM/MeOH. The resulting solid was triturated from MeOH and collected by vacuum filtration to afford **72** (72 mg, 62% yield) as a colorless amorphous solid. MS (ESI pos ion) *m/z*: 527 ($M + H^+$). ^{1}H NMR (400 MHz, DMSO-d_6, δ): 12.45 (s, 1H), 10.60 (br s, 1H), 8.66 (d, *J* = 2.25 Hz, 1H), 8.07 (d, *J* = 2.35 Hz, 1H), 8.05−7.98 (m, 2H), 7.81−7.92 (m, 3H), 7.71 (dd, *J* = 8.46, 1.91 Hz, 1H), 2.22 (s, 3H).

***N*-(6-(6-Chloro-5-(3-(trifluoromethyl)phenylsulfonamido) pyridin-3-yl)benzo[*d*]thiazol-2-yl)acetamide (73).** This material was prepared using an analogous procedure as was used for the preparation of **75**. For the Suzuki step, microwave heating at 100 °C with 100 W of power was used for 10 min. In addition, Cs_2CO_3 was used instead of Na_2CO_3. MS (ESI pos ion) *m/z*: 527 ($M + H^+$). ^{1}H NMR (400 MHz, DMSO-d_6, δ): 12.39 (s, 1H), 8.08−7.99 (m, 3H), 7.91−7.62 (m, 5H), 7.46 (d, *J* = 7.53 Hz, 1H), 2.21 (s, 3H).

***N*-(6-(5-(3-*tert*-Butylphenylsulfonamido)-6-chloropyridin-3-yl)benzo[*d*]thiazol-2-yl)acetamide (78).** Using 3-(*tert*-butyl) benzene-1-sulfonyl chloride and following the procedure used to prepare **75** gave **78** in 99% yield for the sulfonylation step and 18% yield for the Suzuki step. For the Suzuki step, microwave heating at 100 °C with 100 W of power was used for 10 min. In addition, Cs_2CO_3 was used instead of Na_2CO_3. MS (ESI pos ion) *m/z*: 515 ($M + H^+$). ^{1}H NMR (400 MHz, DMSO-d_6, δ): 12.46 (s, 1H), 10.37 (br s, 1H), 8.58 (s, 1H), 8.27 (s, 1H), 7.92 (s, 1H), 7.82 (d, *J* = 8.03 Hz, 1H), 7.74−7.67 (m, 2H), 7.64 (d, *J* = 8.03 Hz, 1H), 7.59 (d, *J* = 7.03 Hz, 1H), 7.54−7.46 (m, 1H), 2.22 (s, 3H), 1.22 (s, 9H).

***N*-(6-(6-Chloro-5-(2-fluorophenylsulfonamido)pyridin-3-yl) benzo[*d*]thiazol-2-yl)acetamide (80).** Using 2-fluorobenzene-1-sulfonyl chloride and following the procedure used to prepare **75** gave **80** in 87% yield for the sulfonylation step and 61% yield for the Suzuki step. For the Suzuki coupling, microwave irradiation at 140 °C for 5 min was used. The crude material from the Suzuki step was purified by MPLC (Teledine ISCO Combiflash Companion) following the procedure outlined for compound **72**. The final compound was purified via trituration from DCM and filtration. MS (ESI pos ion) *m/z*: 477 ($M + H^+$). 1H NMR (400 MHz, DMSO-d_6, δ): 12.45 (s, 1H), 10.79 (br s, 1H), 8.65 (d, *J* = 2.05 Hz, 1H), 8.36 (d, *J* = 1.66 Hz, 1H), 8.09 (s, 1H), 7.85 (d, *J* = 8.41 Hz, 1H), 7.81−7.69 (m, 3H), 7.47 (dd, *J* = 10.03, 8.46 Hz, 1H), 7.40−7.32 (m, 1H), 2.24 (s, 3H).

Procedure for the Synthesis of 71, 74, 76, 77, 79, 81, and 82. *N*-(6-(6-Chloro-5-(phenylsulfonamido)pyridin-3-yl)benzo-[*d*]thiazol-2-yl)acetamide (71). Compound **69** (1.00 g, 4.82 mmol), compound **4a** (1.73 g, 5.45 mmol), $Pd(PPh_3)_4$ (0.836 g, 0.723 mmol), and K_2CO_3 (2.20 g, 15.9 mmol) were suspended in 1,4-dioxane (25 mL), and H_2O (2.5 mL) was added. Argon was bubbled through the suspension for 30 s, and the flask was fitted with a reflux condenser and was placed in a preheated oil bath (100 °C). The mixture was stirred under an inert atmosphere. The mixture was cooled to room temperature after 3 h and then was diluted with DCM and saturated $NaHCO_3$. The organic layer was extracted with DCM (3 × 30 mL), and the organic phases were combined, dried over Na_2SO_4, filtered, and concentrated. The residue was diluted with EtOAc and the precipitate was collected by filtration and washed with hexanes to give the intermediate *N*-(6-(5-amino-6-chloropyridin-3-yl)benzo[*d*]thiazol-2-yl)acetamide (0.500 g, 32.5% yield) as a brown crystalline solid. MS (ESI pos ion) *m/z*: 319 ($M + H^+$). ^{1}H NMR (400 MHz, DMSO-d_6, δ): 12.41 (br s, 1H), 8.24 (s, 1H), 7.94 (s, 1H), 7.81 (d, *J* = 8.53 Hz, 1H), 7.65 (d, *J* = 8.03 Hz, 1H), 7.42 (s, 1H), 5.66 (s, 2H), 2.22 (s, 3H).

Then a 50 mL round-bottomed flask equipped with stir bar was charged with *N*-(6-(5-amino-6-chloropyridin-3-yl)benzo[*d*]thiazol-2-yl)acetamide (50 mg, 0.16 mmol) and THF (1.5 mL). Benzenesulfonyl chloride (0.30 mL, 2.4 mmol), DMAP (1.1 mg, 0.0094 mmol), and pyridine (1.0 mL, 13 mmol) were added. The mixture was allowed to stir under an inert atmosphere at ambient temperature until LCMS analysis indicated that the product was present. The mixture was diluted with DCM and saturated $NaHCO_3$ and then was extracted with DCM (3 × 25 mL). The organics were combined, dried over Na_2SO_4, filtered, concentrated, and purified by ISCO silica gel chromatography in a gradient of 10% → 50% EtOAc/DCM over 35 min to afford **71** (50 mg, 69% yield) as a white crystalline solid. MS (ESI pos ion) *m/z*: 459 ($M + H^+$). ^{1}H NMR (400 MHz, DMSO-d_6, δ): 12.46 (s, 1H), 10.44 (br s, 1H), 8.61 (d, *J* = 2.01 Hz, 1H), 8.32 (d, *J* = 1.51 Hz, 1H), 7.99 (d, *J* = 2.51 Hz, 1H), 7.84 (d, *J* = 8.53 Hz, 1H), 7.79−7.74 (m, 2H), 7.70−7.64 (m, 2H), 7.62−7.56 (m, 2H), 2.23 (s, 3H).

***N*-(6-(6-Chloro-5-(4-(trifluoromethyl)phenylsulfonamido) pyridin-3-yl)benzo[*d*]thiazol-2-yl)acetamide (74).** Using 4-(trifluoromethyl)benzenesulfonyl chloride and following the procedure used to prepare **71** gave **74** in 8% yield. To isolate the crude material, H_2O was added, and the mixture was stirred at room temperature for 1 h. The resultant precipitate was collected by filtration and purified by ISCO silica gel chromatography in a gradient of 1% → 10% MeOH/DCM over 35 min. MS (ESI pos ion) *m/z*: 527 ($M + H^+$). ^{1}H NMR (400 MHz, DMSO-d_6, δ): 12.42 (br s, 1H), 8.54 (d, *J* = 1.51 Hz, 1H), 8.24 (d, *J* = 1.51 Hz, 1H), 8.01−7.99 (m, 5H), 7.81 (d, *J* = 8.53 Hz, 1H), 7.65 (dd, *J* = 8.53, 1.51 Hz, 1H), 2.22 (s, 3H).

***N*-(6-(6-Chloro-5-(3-chlorophenylsulfonamido)pyridin-3-yl)benzo[*d*]thiazol-2-yl)acetamide (76).** Using 3-chlorobenzenesulfonyl chloride and following the procedure used to prepare **71** gave **76** in 19% yield. MS (ESI pos ion) *m/z*: 493 ($M + H^+$). ^{1}H NMR (400 MHz, DMSO-d_6, δ): 12.46 (s, 1H), 10.64 (br s, 1H), 8.34 (s, 1H), 8.02 (d, *J* = 2.01 Hz, 1H), 7.84 (d, *J* = 8.53 Hz, 1H), 7.81−7.75 (m, 2H), 7.74−7.67 (m, 2H), 7.65−7.59 (m, 1H), 2.23 (s, 3H).

***N*-(6-(6-Chloro-5-(4-chlorophenylsulfonamido)pyridin-3-yl)benzo[*d*]thiazol-2-yl)acetamide (77).** Using 4-chlorobenzenesulfonyl chloride and following the procedure used to prepare **71** gave **77** in 24% yield. The following modifications were made: The sulfonylation reaction was run using only pyridine as the solvent, and the final compound was purified by ISCO silica gel chromatography using a gradient of 0% → 10% MeOH/DCM over 30 min. MS (ESI pos ion) *m/z*: 493 ($M + H^+$). ^{1}H NMR (400 MHz, DMSO-d_6, δ): 12.46 (s, 1H), 10.57 (br s, 1H), 8.63 (s, 1H), 8.33 (s, 1H), 8.02 (s, 1H), 7.84 (d, *J* = 8.03 Hz, 1H), 7.79−7.64 (m, 5H), 2.23 (s, 3H).

***N*-(6-(6-Chloro-5-(4-*tert*-butylphenylsulfonamido)pyridin-3-yl)benzo[*d*]thiazol-2-yl)acetamide (79).** Using 4-*tert*-butylbenzenesulfonyl chloride and following the procedure used to prepare **71** gave **79** in 16% yield. MS (ESI pos ion) *m/z*: 515 ($M + H^+$). ^{1}H

NMR (400 MHz, DMSO-d_6, δ): 12.39 (s, 1H), 7.94 (br s, 1H), 7.78−7.70 (m, 2H), 7.68 (d, J = 8.53 Hz, 2H), 7.63 (br s, 1H), 7.45−7.37 (m, 3H), 2.21 (s, 3H), 1.26 (s, 9H).

***N*-(6-(6-Chloro-5-(3-fluorophenylsulfonamido)pyridin-3-yl)benzo[*d*]thiazol-2-yl)acetamide (81).** Using 3-fluorobenzenesulfonyl chloride and following the procedure used to prepare **71** gave **81** in 40% yield. MS (ESI pos ion) m/z: 477 ($M + H^+$). ^{1}H NMR (400 MHz, DMSO-d_6, δ): 12.46 (s, 1H), 10.62 (br s, 1H), 8.62 (d, J = 1.51 Hz, 1H), 8.34 (s, 1H), 8.02 (d, J = 1.51 Hz, 1H), 7.84 (d, J = 8.53 Hz, 1H), 7.71 (d, J = 8.03 Hz, 1H), 7.67−7.57 (m, 4H), 2.22 (s, 3H).

***N*-(6-(6-Chloro-5-(4-fluorophenylsulfonamido)pyridin-3-yl)benzo[*d*]thiazol-2-yl)acetamide (82).** Using 4-fluorobenzenesulfonyl chloride and following the procedure used to prepare **71** gave **82** in 57% yield. The following modifications were made: The sulfonylation reaction was run using only pyridine as the solvent, and crude product was collected by treating the mixture with H_2O and filtering the resulting suspension. The solid was washed with H_2O and EtOAc and recrystallized from MeOH to afford **82** as a white powder. MS (ESI pos ion) m/z: 477 ($M + H^+$). ^{1}H NMR (300 MHz, DMSO-d_6, δ): 12.47 (s, 1H), 10.50 (br s, 1H), 8.64 (d, J = 2.34 Hz, 1H), 8.35 (d, J = 1.61 Hz, 1H), 8.04 (d, J = 2.34 Hz, 1H), 7.88−7.78 (m, 3H), 7.72 (dd, J = 8.48, 1.90 Hz, 1H), 7.48−7.40 (m, 2H), 2.23 (s, 3H).

In Vitro Assays. PI3K Enzyme Assay. Human p110-α, -β, and -δ with N-terminal poly-His tags were coexpressed with p85-α in a Sf9 baculovirus expression system. p110-δ/p85 heterodimers were purified by sequential Ni-NTA, Q-HP, Superdex-100 chromatography. A truncated form of PI3Kγ encompassing residues 114−1102, N-terminally labeled with poly-His tag, was expressed with baculovirus in Hi5 insect cells and purified by sequential Ni-NTA, Superdex-200, Q-HP chromatography.

The inhibition of PI3K activity was determined using a modified in vitro AlphaScreen assay.[59] From a starting concentration of 5 mM, test compounds were serially diluted 1:2 across 384-well Greiner clear polypropylene plates (supplier) to yield 22 test concentrations. Columns 23 and 24 contained only DMSO and were designated for positive and negative controls. Source plates were replicated into 384-well Optiplates (PerkinElmer, Waltham, MA), 0.5 μL/well, to make assay-ready plates. PI3K enzyme was diluted in enzyme reaction buffer (50 mM Tris-HCl, pH 7, 14 mM $MgCl_2$, 2 mM sodium cholate, 100 mM NaCl, and 2 mM DTT) to give 2× working solutions. PI3Kα and PI3Kδ were diluted to 1.6 nM. PI3Kβ was diluted to 0.8 nM, and PI3Kγ was diluted to a final concentration of 15 nM. 2× substrate solutions containing 10 μM PI(4,5)P2 (Echelon Biosciences, Salt Lake City, UT) were generated containing either 20 μM ATP, used in the assays testing PI3Kα and PI3Kβ, or 8 μM ATP used in the assays testing PI3Kγ and PI3Kδ. By use of a 384-well dispensing Multidrop (Titertek, Huntsville, AL), 10 μL of 2× enzyme reaction mixture and 10 μL of the appropriate substrate solution were then added to columns 1−24 of the 384-well containing serially diluted test compound. Plates were then incubated at room temperature for 20 min.

The reaction was subsequently terminated by the addition of 10 μL/well of the donor bead solution composed of 40 nM biotinylated-IP_4 (Echelon Biosciences, Salt Lake City, UT), 80 μg/mL streptavadin-donor beads diluted in AlphaScreen reaction buffer (10 mM Tris-HCl, pH 7.5, 150 mM NaCl, 0.10% Tween 20, and 30 mM EDTA). The plates were incubated at room temperature in the dark for 30 min. Then 10 μL of the acceptor bead solution, containing 40 nM PIP_3-binding protein (Echelon Biosciences, Salt Lake City, UT) and 80 μg/mL anti-GST-acceptor beads diluted in α screen reaction buffer, was then added to each well. The plates were then incubated in the dark for an additional 1.5 h prior to being read on an Envision multimode plate reader (PerkinElmer, Waltham, MA) with a 680 nm excitation filter and a 520−620 nm emission filter. IC_{50} determinations were analyzed using the Genedata Screener (ALDI) high content data analysis program nonlinear regression Hill equations.

mTOR LanthaScreen Assay. The mTOR LanthaScreen is a TR-FRET assay measuring the phosphorylation of mTOR's substrate 4EBP1. The 384-well compound plates were prepared by Amgen's sample bank containing 1 μL of compound per well starting at 5 mM and diluted 1:2 across the row, resulting in a 22-well serial dilution. Then 24 μL of assay buffer (Invitrogen, PV4794) with 2 mM DTT was added to the compound plate in rows 1−24 using the VELOCITY11 VPREP 384 ST, resulting in a DMSO concentration of 4%. The compound plate was mixed, and 2.5 μL of serially diluted compound or controls was added to the assay plate (Costar, 3658).

The assay was conducted on the PerkinElmer FlexDrop PLUS. A 5 μL mix of 800 nM GFP-4E-BP1 (Invitrogen, PV4759) and 20 μM ATP (Amgen) was added to rows 1−24. Then 2.5 μL of 0.6 μg/mL of recombinant mTOR (Amgen, N-terminal GST-tagged mTOR fragment spanning amino acids 1360−2549) was added to rows 1−23. An amount of 2.5 μL of assay buffer was added to row 24 for the low control. The final concentration of the compounds was 50 μM serially diluted to 23.84 pM in 1% DMSO. The final high control had 1% DMSO, and the low control was a no enzyme control with a concentration of 1% DMSO. The final concentrations of the assay reagents were 400 nM GFP-4E-BP1, 10 μM of ATP, and 0.15 μg/mL mTOR enzyme. Compound, enzyme, and substrate were incubated for 90 min. At this point, 10 μL of stop solution was added (20 mM Tris, pH 7.5 (Invitrogen, 15567-027), 0.02% sodium azide (Teknova, S0208), 0.01% NP-40 (Roche, 11754599001), 20 mM EDTA (Invitrogen, 15575-038), and 4 nM Tb-anti-p4E-BP1 (Invitrogen, PV4758)) for a final concentration of 2 nM Tb-anti-p4E-BP1. The mixtures were then incubated for 60 min.

The plates were read on the PerkinElmer EnVision 2103 multilable reader using the excitation filter 340 nm and the emission filters 520 and 495 nm. The ratio of 520 nm/495 nm was calculated, and the POC data were analyzed to report the IC_{50} IP for the phosphorylation of 4EBP1. IC_{50} values were determined by Genedata Screener software using an Amgen designed fit strategy.

DNA-PK LanthaScreen Enzyme Assay. IC_{50} values for the inhibition of the DNA-PK were measured using a LanthaScreen TR-FRET enzyme assay. The enzyme assay was carried out in 384-well polystyrene low volume plates. All reagents were diluted in kinase buffer (50 mM HEPES (pH 7.5), 10 mM $MgCl_2$, 1 mM EGTA, 0.01% Brij-35, and 1 mM DTT). The 3-fold, 10-point serial compound dilutions (4×) were prepared in kinase buffer (20% DMSO) with a top concentration of 12 μM and aliquoted into assay plates in 2.5 μL/well volumes. A 4× substrate working stock solution containing 44 μM ATP, 1600 nM fluorescein-p53 [Ser15] peptide (Invitrogen, PV5132), and 10 μg/mL sheared calf thymus DNA (Invitrogen, 15633-019) was prepared in kinase buffer and aliquoted into the assay plate in 2.5 μL/well volumes. The reaction was initiated by adding 5 μL/well of a 2× enzyme working stock solution containing 2 U/μL of DNA-PK enzyme (Promega, 9PIV581) prepared in kinase buffer. The enzyme reaction was carried out for 30 min before being terminated by adding 10 μL/well of a 2× termination solution containing 20 mM EDTA and 4 nM Tb-anti-phospho-p53(S15) Ab (Invitrogen, PV5130) solution. The assay plate was then incubated at room temperature for 1 h and read on a Tecan Safire II. IC_{50} values were determined by Genedata Screener software using an Amgen designed fit strategy.

hVPS34 LanthaScreen Enzyme Assay. IC_{50} values for the inhibition of hVPS34 were measured using a fluorescence-based immunoassay for the detection of ADP (Adapta universal kinase assay kit, Invitrogen, PV5099). The enzyme assay was carried out in 384-well polystyrene low volume plates. All reagents were diluted in kinase buffer (50 mM HEPES (pH 7.5), 0.1% CHAPS, 1 mM EGTA, 2 mM $MnCl_2$, 2 mM DTT). The 3-fold, 10-point serial compound dilutions (4×) were prepared in kinase buffer (4% DMSO) with a top concentration of 36 μM and aliquoted into assay plates in 2.5 μL/well volumes.

A 4× enzyme working solution was prepared by diluting hVPS34 (Invitrogen, PV5126) in kinase buffer to 650 μg/mL and aliquoted into assay plates in 2.5 μL/well volumes. The reaction was initiated by adding 5 μL/well of a 2× substrate working stock solution containing 200 μM phosphatidylinositol/phosphatidylserine (Invitrogen, PV5122) and 20 μM ATP. The enzyme reaction was carried out at room temperature for 30 min before being terminated with 5 μL/well of kinase quench buffer containing 30 mM EDTA, 6 nM ADP-Ab, and 15 nM ADP-tracer. The assay plate was then incubated at room temperature for 30 min and read on a Tecan Safire II. IC_{50} values were determined by Genedata Screener software using an Amgen designed fit strategy.

Akt (Ser 473) Phosphorylation Cell Based Assay. U-87 MG cells diluted to 0.25 million cells/mL were plated at 20 μL per well in 384-well white tissue culture plates. The plates were then incubated overnight at 37 °C at 5% CO_2 in MEM supplemented with 10% FBS, nonessential amino acids, and L-glutamine (all purchased from Gibco, Carlsbad, CA).

The 384-well compound plates were prepared containing 1 μL of compound per well at a starting concentration of 5 mM and diluted 1:2 to produce a 22-well serial dilution. Then 39 μL of growth medium was added to the compound plate in rows 1−22 using the PerkinElmer FlexDrop PLUS, resulting in a DMSO concentration of 2.5%. The cell plates and diluted compound plates were put onto the VELOCITY11 VPREP 384 ST where the compound plate was mixed, and 5 μL of serially diluted compound or controls was added to the cell plate. The final concentration of the compounds was 25 μM serially diluted to 11.9 pM in 0.5% DMSO. The cell plates were then incubated with compound for 2 h at 37 °C, 5% CO_2. After 2 h, the medium in the cell plates was aspirated using the BioTek ELx405HT plate washer (Winooski, VT), removing most of the medium and compound without disturbing the adherent U-87 MG cells.

Akt (Ser 473) phosphorylation was determined using a SureFire Akt (Ser 473) phosphorylation (TGR BioSciences, Adelaide, Austalia) and IgG detection kits (PerkinElmer, Waltham, MA). An amount of 5 μL of 1× lysis buffer was added to each well using the PerkinElmer FlexDrop PLUS. The plates were then incubated at room temperature on a shaker for 10 min. The AlphaScreen reaction was then prepared under low light conditions (subdued or green light) containing p-Akt(Ser 473) reaction buffer, dilution buffer, activation buffer, acceptor beads, and donor beads at a ratio of 40:20:10:1:1, respectively. The AlphaScreen reaction was added to the cell lysate at 6 μL per well using the PerkinElmer FlexDrop PLUS. The plates were placed in a humid environment to reduce edge effects and incubated overnight at room temperature with restricted air flow in the dark. The plates were read on the PerkinElmer EnVision 2103 multilable reader using the standard AlphaScreen readout. IC_{50} values were then determined by Genedata Screener software using an Amgen designed fit strategy.

U-87 MG and PC3 Cell Viability Assay. U-87 MG and PC-3 tumor cells were seeded at a density of 3000 cells/well (U-87 MG-growth medium containing MEM supplemented with 10% FBS, 1× nonessential amino acids, and 1× L-glutamine (all purchased from Invitrogen); PC-3 growth medium containing RPMI supplemented with 10% FBS and 1× L-glutamine (all purchased from Invitrogen)) in 96-well tissue culture plates and subsequently incubated overnight at 37 °C and 5% CO_2 to allow cells to adhere to the plate. Ten-point 1:3 serial dilutions of compound **82** were prepared in DMSO and added to cells, covering a dose range of 10 μM to 500 pM. ATPlite one-step viability assays (Perkin-Elmer, 6016731) were carried out following 72 h of compound treatment. IC_{50} IP values were calculated with XLfit (IDBS software), applying a four-parameter logistic model for curve fitting. Mean IC_{50} IP values are reported from a minimum of two experiments.

In Vivo Assays. PD Assay. Four- to five-week old female CD1 nude mice (Charles Rivers Laboratories) were used in all In Vivo studies. For the liver PD assay, mice were dosed orally (via gavage) with compound **82** at different doses as indicated. Three hours after dosing, 0.2 mL of recombinant human HGF (0.06 mg/mL) was administrated through the tail of each mouse (12 μg/mouse). After 5 min, animals were anesthetized and sacrificed and blood samples were collected and placed in heparinized tubes. Blood samples were then centrifuged to obtain the plasma for PK analysis. Liver tissues were harvested and fast-frozen in liquid nitrogen for analysis of Akt (Ser 473) phosphorylation.

For Akt (Ser 473) phosphorylation analysis, each liver was homogenized in 1 mL of ice-cold MSD lysis buffer (containing 150 mM NaCl, 20 mM Tris, pH 7.5, 1 mM EDTA, 1 mM EGTA, 1% Triton-X-100, 1/10 protease inhibitor tablet (Roche, catalog no. 1836170), 20 μL of phosphatase inhibitor I (Sigma-Aldrich, Inc., catalog no. P-2850), 20 μL of phosphatase inhibitor II (Sigma-Aldrich, Inc., catalog no. P-5726) and 40 mM NaF) with GenoGrinder 2000 (BT&C Inc., product no. SP2100-115) at 350 strokes/min for 2 min at room temperature. The lysate was centrifuged (2×) in a 1.5 mL Eppendorf microcentrifuge tube at 14 000 rpm for 15 min at 4 °C. The supernatant was precleared with Protein A/G beads (PIERCE, product no. 20421) in an Eppendorf microcentrifuge tube at 4 °C for 1 h. The beads were centrifuged at 14 000 rpm for 15 min at 4 °C, and the supernatant was transferred to a clean Eppendorf microcentrifuge tube. The protein concentration of each sample was determined using Bio-Rad DC protein assay (Bio-Rad, catalog no. 500-0116) and normalized to a final concentration of 1 mg/mL. The level of phosphorylated Akt(S473) and total Akt in mouse liver lysates were detected using Meso Scale Discovery phospho-Akt(S473) (catalog no. K151CAD-2) and total Akt (catalog no. K151CBD-2) whole cell lysate kits. pAkt(S473) MSD plate and total Akt MSD plate were blocked with 150 μL of MSD blocking solution (containing 3% bovine serum albumin, 50 mM Tris, pH 7.5, 150 mM NaCl, and 0.02% Tween-20) and incubated at room temperature for 1 h. The plates were then washed (4×) with 300 μL of MSD Tris wash buffer (containing 50 mM Tris, pH 7.5, 150 mM NaCl, and 0.02% Tween-20). An amount of 25 μL (1mg / mL) of liver lysate was dispensed to each well of the MSD plate. The plate was incubated with shaking in Eppendorf thermonixer R (Eppendorf, product no. 22670107) at 600 rpm at room temperature for 2 h. The plate was then washed four times with 300 μL of MSD Tris wash buffer. An amount of 25 μL (1.5 μg/mL) of anti-pAkt(S473) or antitotal Akt detection antibody solution was added to each well of the MSD plate. The plate was incubated with shaking in Eppendorf Thermomixer R at 600 rpm at room temperature for 1 h. The plate was then washed (4×) with 300 μL of MSD Tris wash buffer. An amount of 150 μL of 1× MSD read buffer was added to each well of the MSD plate. The intensity of pAkt(S473) or total Akt signal was measured using MSD sector imager 6000.

The raw phosphorylated Akt(S473) values were divided by the ratio of the mean of total Akt in each group in order to adjust the values for phosphorylated Akt(S473) data to account for varying total Akt levels in individual tissue samples. All results were expressed as the mean ± standard error. Statistical analysis was performed by analysis of variance (ANOVA) followed by Bonferroni−Dunn post hoc test.

Xenograft Studies. Mice were injected subcutaneously with 0.2 mL of tumor cell suspension in medium mixed with 1:1 ratio of matrigel (BD Bioscience), which contains 5×10^6 U-87 MG cells (ATCC), 5×10^6 A549 cells (ATCC), or 2×10^6 HCT116 cells (ATCC). Subconfluent cells were harvested prior to injection. Ten to thirteen days after tumor cell inoculation, when the tumor volume had reached ∼200 mm^3, animals were divided randomly into test groups (each with 10 mice), and the daily oral administration of **82** at indicated doses began and continued to the end of each study. Tumor volumes and body weights were recorded at intervals of 3 or 4 days. Tumor volume was calculated as length × width × width/2 and is in mm^3. Results are expressed as the mean ± standard error. The data were statistically analyzed with ANOVA or ANOVA followed by RM-ANOVA for

repeated measurements (JMP 7). Mice were euthanized with CO_2 asphyxiation, and final plasma samples were harvested for PK analysis. All experiments were conducted in accordance with institutional guidelines, which include mandates for sacrificing mice when tumors exceed size thresholds.

Crystallography: Determination of p110γ Crystal Structures. Human p110γ(144−1102) was expressed, purified, and crystallized according to published procedures.[60] Inhibitor complexes were obtained by soaking apo crystals overnight in cryo solutions (mother liquor plus 20% glycerol) containing 1 mM compound. Crystals were then flash-frozen in liquid nitrogen prior to data collection. Diffraction data for p110γ + **1** were collected at the Advanced Photon Source, beamline 31-ID using λ = 0.9793 Å and a MAR 165 mm CCD detector. Diffraction data for p110γ + **82** were collected on a FR-E rotating anode X-ray source equipped with an RAXIS IV++ detector. Data were reduced using the HKL software suite,[61] and the structures were solved by molecular replacement using apo human p110γ as a search model (PDB code 1E8Y). Structures were refined using REFMAC,[62,63] and model building was performed with COOT.[64]

■ ASSOCIATED CONTENT

Supporting Information. Synthetic methods used for analogues **14**−**45**, X-ray data for **1** and **82**, enzyme selectivity data for **82**, analytical HPLC methods, and PD data for compound **73**. This material is available free of charge via the Internet at http://pubs.acs.org.

■ AUTHOR INFORMATION

Corresponding Author

*Telephone: 805-313-6550. Fax: 805-480-3016. E-mail: dangelo@amgen.com.

■ ACKNOWLEDGMENT

We thank Teresa Burgess, Randall Hungate, Richard Kendall, Robert Radinsky, and Terry Rosen for their support and direction of this work. We also thank Yunxin Bo, Derin D'Amico, Lillian Liao, Philip Olivieri, and Emily Peterson for their contributions of specific compounds and intermediates to this manuscript. Finally, we thank Paul Andrews for his support with the cellular assay.

■ ABBREVIATIONS USED

Ac, acetyl; AKT, serine−threonine kinase Akt; DCM, dichloromethane; DMAP, 4-dimethylaminopyridine; DME, 1,2-dimethoxyethane; DMF, *N*,*N*-dimethylformamide; DMSO, dimethylsulfoxide; EC, effective concentration; ED, effective dose; HGF, hepatocyte growth factor; HLM, human liver microsomes; iv, intravenous; mTOR, mammalian target of rapamycin; PD, pharmacodynamic; PIP2, phosphatidylinositol 4,5-biphosphate; PIP3, phosphatidylinositol 3,4,5-triphosphate; PI3K, phosphoinositide 3-kinase; PK, pharmacokinetic; PTEN, phosphatase and tensin homologue gene; RLM, rat liver microsomes; SAR, structure−activity relationship; TFA, trifluoroacetic acid; TFE, trifluoroethanol; THF, tetrahydrofuran; Xantphos, 4,5-bis(diphenylphosphino)-9,9-dimethylxanthene

■ REFERENCES

(1) Engleman, J. A.; Luo, J.; Cantley, L. C. The Evolution of Phosphatidylinositol 3-Kinases as Regulators of Growth and Metabolism. *Nat. Rev. Genet.* **2006**, *7*, 606–619.

(2) Marone, R.; Cmiljanovic, V.; Giese, B.; Wymann, M. P. Targeting Phosphoinositide 3-Kinase: Moving towards Therapy. *Biochim. Biophys. Acta* **2008**, 159–185.

(3) Liu, P.; Cheng, H.; Roberts, T. M.; Zhao, J. J. Targeting the Phosphoinositide 3-Kinase Pathway in Cancer. *Nat. Rev. Drug Discovery* **2009**, *8*, 627–644.

(4) Franke, T. F.; Kaplan, D. R.; Cantley, L. C. PI3K: Downstream AKTion Blocks Apoptosis. *Cell* **1997**, *88*, 435–437.

(5) Shepherd, P. R.; Withers, D. J.; Siddle, K. Phosphoinositide 3-Kinase: The Key Switch Mechanism in Insulin Signaling. *Biochem. J.* **1998**, *333* (Part 3), 471–490.

(6) Maehama, T.; Dixon, J. E. The Tumor Suppressor, PTEN/MMAC1, Dephosphorylates the Lipid Second Messenger, Phosphatidylinositol 3,4,5-Triphosphate. *J. Biol. Chem.* **1998**, *273*, 13375–13378.

(7) Maehama, T.; Taylor, G. S.; Dixon, J. E. PTEN and Myotubularin: Novel Phosphoinositide Phosphatases. *Annu. Rev. Biochem.* **2001**, *70*, 247–279.

(8) Vivanco, I.; Sawyers, C. L. The Phosphatidylinositol 3-Kinase-AKT Pathway in Human Cancer. *Nat. Rev. Cancer* **2002**, *2*, 489–501.

(9) Wishart, M. J.; Dixon, J. E. PTEN and Myotubularin Phosphatases: From 3-Phosphoinositide Dephosphorylation to Disease. *Trends Cell Biol.* **2002**, *12*, 579–585.

(10) Bader, A. G.; Kang, S.; Zhao, L.; Vogt, P. K. Oncogenic PI3K Deregulates Transcription and Translation. *Nat. Rev. Cancer* **2005**, *5*, 921–929.

(11) Manning, B. D.; Cantley, L. C. AKT/PKB Signaling: Navigating Downstream. *Cell* **2007**, *129*, 1261–1274.

(12) Janssen, J. W.; Schleithoff, L.; Bartram, C. R.; Schulz, A. S. An Oncogenic Fusion Product of the Phosphatidylinositol 3-Kinase p85β Subunit and HUMORF8, a Putative Deubiquitinating Enzyme. *Oncogene* **1998**, *16*, 1767–1772.

(13) Jimenez, C.; Jones, D. R.; Rodriguez-Viciana, P.; Gonzalez-Garcia, A.; Leonardo, E.; Wennstrom, S.; von Kobbe, C.; Toran, J. L.; R.-Borlado, L.; Calvo, V.; Copin, S. G.; Albar, J. P.; Gaspar, M. L.; Diez, E.; Marcos, M. A. R.; Downward, J.; Martinez-A., C.; Merida, I.; Carrera, A. C. Identification and Characterization of a New Oncogene Derived from the Regulatory Subunit of Phosphoinositide 3-Kinase. *EMBO J.* **1998**, *17*, 743–753.

(14) Jucker, M.; Sudel, K.; Horn, S.; Sickel, M.; Wegner, W.; Fiedler, W.; Feldman, R. A. Expression of a Mutated Form of the p85α Regulatory Subunit of Phosphatidylinositol 3-Kinase in a Hodgkin's Lymphona-Derived Cell Line (CO). *Leukemia* **2002**, *16*, 894–901.

(15) Samuels, Y.; Wang, Z.; Bardelli, A.; Silliman, N.; Ptak, J.; Szabo, S.; Yan, H.; Gazdar, A.; Powell, S. M.; Riggins, G. J.; Willson, J. K. V.; Markowitz, S.; Kinzler, K. W.; Vogelstein, B.; Velculescu, V. E. High Frequency of Mutations of the PIK3CA Gene in Human Cancers. *Science* **2004**, *304*, 554.

(16) Isakoff, S. J.; Engelman, J. A.; Irie, H. Y.; Luo, J.; Brachmann, S. M.; Pearline, R. V.; Cantley, L. C.; Brugge, J. S. Breast Cancer-Associated PIK3CA Mutations Are Oncogenic in Mammary Epithelial Cells. *Cancer Res.* **2005**, *65*, 10992–11000.

(17) Kang, S.; Bader, A. G.; Vogt, P. K. Phosphatidylinositol 3-Kinase Mutations Identified in Human Cancer Are Oncogenic. *Proc. Natl. Acad. Sci. U.S.A.* **2005**, *102*, 802–807.

(18) Samuels, Y.; Diaz, L. A.; Schmidt-Kittler, O.; Cummins, J. M.; DeLong, L.; Cheong, I.; Rago, C.; Huso, D. L.; Lengauer, C.; Kinzler, K. W.; Vogelstein, B.; Velculescu, V. E. Mutant PIK3CA Promotes Cell Growth and Invasion of Human Cancer Cells. *Cancer Cell* **2005**, *7*, 561–573.

(19) Shayesteh, L.; Lu, Y.; Kuo, W. L.; Baldocchi, R.; Godfrey, T.; Collins, C.; Pinkel, D.; Powell, B.; Mills, G. B.; Gray, J. W. PIK3CA Is Implicated as an Oncogene in Ovarian Cancer. *Nat. Genet.* **1999**, *21*, 99–102.

(20) Borlado, L. R.; Redondo, C.; Alvarez, B.; Jimenez, C.; Criado, L. M.; Flores, J.; Marcos, M. A. R.; Martinez-A, C.; Balomenos, D.; Carrera, A. C. Increased Phosphoinositide 3-Kinase Activity Induces a Lymphoproliferative Disorder and Contributes to Tumor Generation In Vivo. *FASEB J.* **2000**, *14*, 895–903.

(21) Ma, Y. T.; Wei, S. J.; Lin, Y. C.; Lung, J. C.; Chang, T. C.; Whang-Peng, J.; Liu, J. M.; Yang, D. M.; Yang, W. K.; Shen, C. Y. PIK3CA as an Oncogene in Cervical Cancer. *Oncogene* **2000**, *19*, 2739–2744.

(22) Trotman, L. C.; Niki, M.; Dotan, Z. A.; Koutcher, J. A.; Di Cristofano, A.; Xiao, A.; Khoo, A. S.; Roy-Burman, P.; Greenbert, N. M.; Dyke, T. V.; Cordon-Cardo, C.; Pandolfi, P. P. PTEN Dose Dictates Cancer Progression in the Prostate. *PLoS Biol.* **2003**, *1* (3), 385–396.

(23) Leslie, N. R.; Downes, C. P. PTEN Function: How Normal Cells Control It and Tumour Cells Lose It. *Biochem. J.* **2004**, *382*, 1–11.

(24) Parsons, R. Human Cancer, PTEN, and the PI-3 Kinase Pathway. *Semin. Cell Dev. Biol.* **2004**, *15*, 171–176.

(25) Cully, M.; You, H.; Levine, A. J.; Mak, T. W. Beyond PTEN Mutations: The PI3K Pathway as an Integrator of Multiple Inputs During Tumorigenesis. *Nat. Rev. Cancer* **2006**, *6*, 184–192.

(26) Guertin, D. A.; Sabatini, D. M. Defining the Role of mTOR in Cancer. *Cancer Cell* **2007**, *12*, 9–22.

(27) Karakas, B.; Bachman, K. E.; Park, B. H. Mutation of the PIK3CA Oncogene in Human Cancers. *Br. J. Cancer* **2006**, *94*, 455–459.

(28) Vogt, P. K.; Kang, S.; Elsliger, M. A.; Gymnopoulos, M. Cancer-Specific Mutations in Phosphatidylinositol 3-Kinase. *Trends Biochem. Sci.* **2007**, *32*, 342–349.

(29) Yap, T. A.; Garrett, M. D.; Walton, M. I.; Raynaud, F.; De Bono, J. S.; Workman, P. Targeting the PI3K-AKT-mTOR Pathway: Progress, Pitfalls, and Promises. *Curr. Opin. Pharmacol.* **2008**, *8*, 393–412.

(30) Kong, D.; Yamori, T. Advances in Development of Phosphatidylinositol 3-Kinase Inhibitors. *Curr. Med. Chem.* **2009**, *16*, 2839–2854.

(31) Fan, Q. W.; Knight, Z. A.; Goldenberg, D. D.; Yu, W.; Mostov, K. E.; Stokoe, D.; Shokat, K. M.; Weiss, W. A. A Dual PI3 Kinase/mTOR Inhibitor Reveals Emergent Efficacy in Glioma. *Cancer Cell* **2006**, *9*, 341–349.

(32) Ihle, N. T.; Powis, G. Inhibitors of Phosphatidylinositol-3-kinase in Cancer Therapy. *Mol. Aspects. Med.* **2010**, *31*, 135–144.

(33) Knight, S. D.; Adams, N. D.; Burgess, J. L.; Chaudhari, A. M.; Darcy, M. G.; Donatelli, C. A.; Luengo, J. I.; Newlander, K. A.; Parrish, C. A.; Ridgers, L. H.; Sarpong, M. A.; Schmidt, S. J.; Van Aller, G. S.; Carson, J. D.; Diamond, M. A.; Elkins, P. A.; Gardiner, C. M.; Garver, E.; Gilbert, S. A.; Gontarek, R. R.; Jackson, J. R.; Kershner, K. L.; Luo, L.; Raha, K.; Sherk, C. S.; Sung, C. M.; Sutton, D.; Tummino, P. J.; Wegrzyn, R. J.; Auger, K. R.; Dhanak, D. Discovery of GSK2126458, a Highly Potent Inhibitor of PI3K and the Mammalian Target of Rapamycin. *ACS Med. Chem. Lett.* **2010**, *1*, 39–43.

(34) Knight, Z. A.; Gonzalez, B.; Feldman, M. E.; Zunder, E. R.; Goldenberg, D. D.; Williams, O.; Loewith, R.; Stokoe, D.; Balla, A.; Toth, B.; Balla, T.; Weiss, W. A.; Williams, R. L.; Shokat, K. M. A Pharmacological Map of the PI3-K Family Defines a Role of p110α in Insulin Signaling. *Cell* **2006**, *125*, 733–747.

(35) At the time of these studies, the X-ray crystal structure of PI3Kα had yet to be realized, though it has since been reported: Huang, C. H.; Mandelker, D.; Schmidt-Kittler, O.; Samuels, Y.; Velculescu, V. E.; Kinzler, K. W.; Vogelstein, B.; Gabelli, S. B.; Amzel, M. The Structure of a Human p110α/p85α Complex Elucidates the Effects of Oncogenic PI3Kα Mutations. *Science* **2007**, *318*, 1744–1748.

(36) Suzuki, A. Recent Advances in the Cross-Coupling Reactions of Organoboron Derivatives with Organic Electrophiles, 1995−1998. *J. Organomet. Chem.* **1999**, *576*, 147–168 and references therein.

(37) Molander, G. A.; Biolatto, B. Efficient Ligandless Palladium-Catalyzed Suzuki Reactions of Potassium Aryltrifluoroborates. *Org. Lett.* **2002**, *4* (11), 1867–1870.

(38) Molander, G. A.; Biolatto, B. Palladium-Catalyzed Suzuki−Miyaura Cross-Coupling Reactions of Potassium Aryl- and Heteroaryltrifluoroborates. *J. Org. Chem.* **2003**, *68* (11), 4302–4314.

(39) Darses, S.; Genet, J. P. Potassium Organotrifluoroborates: New Perspectives in Organic Synthesis. *Chem. Rev.* **2008**, *108*, 288–325.

(40) Negishi, E.; King, A. O.; Okukado, N. J. Selective Carbon−Carbon Bond Formation via Transition Metal Catalysis. 3. A Highly Selective Synthesis of Unsymmetrical Biaryls and Diarylmethanes by the Nickel- or Palladium-Catalyzed Reaction of Aryl- and Benzylzinc Derivatives with Aryl Halides. *J. Org. Chem.* **1977**, *42*, 1821–1823.

(41) For preparation of *N*-ethyl-4-methoxybenzenesulfonamide (used to prepare **39**) and 2-fluoro-*N*-methylbenzenesulfonamide (used to prepare **41**), the following reference should be consulted: Booker, S. K.; D'Angelo, N. D.; D'Amico, D. C.; Kim, T. S.; Liu, L.; Meagher, K.; Norman, M. H.; Panter, K.; Schenkel, L. B.; Smith, A. L.; Tamayo, N. A.; Whittington, D. A.; Xi, N.; Yang, K. Preparation of 2-Aminobenzothiazole Derivatives as Phosphoinositide 3-Kinase (PI3 Kinase) Modulators. PCT Int. Appl. WO2009017822A2, 2009.

(42) Jones, C. D.; Luke, R. W. A.; Mccoull, W. Preparation of Ethynylpyrimidine Derivatives as Tie2 Receptor Tyrosine Kinase Inhibitors for the Treatment of Cancer. PCT Int. Appl. WO2006-103449A2, 2006.

(43) An X-ray structure of 2-phenoxypyrimidine (analogous to **8**) revealed a dihedral angle of 76−79° between the two ring planes (Bakhtiar, N. S.; Abdullah, Z.; Ng, S. W. 2-Phenoxypyrimidine. *Acta Crystallogr., Sect. E* **2009**, *65*, o114), while an X-ray structure of *N*-(pyrimidine-2-yl)aniline (analogous to **10**) showed a dihedral angle of 31−35° (Badaruddin, E.; Bakhtiar, N. S.; Aiyub, Z.; Abdullah, Z.; Ng, S. W. *N*-(Pyrimidin-2-yl)aniline. *Acta Crystallogr. Sect. E* **2009**, *65*, o703).

(44) Bengtsson, M.; Larsson, J.; Nikitidis, G.; Storm, P.; Bailey, J. P.; Griffen, E. J.; Arnould, J. C.; Bird, T. G. C. 5-Heteroaryl Thiazoles and Their Use as PI3K Inhibitors. PCT Int. Appl. WO2006051270A1, 2006.

(45) Arnould, J. C.; Foote, K. M.; Griffen, E. J. Thiazole Derivates and Their Use as Anti-Tumour Agents. PCT Int. Appl. WO2007-129044A1, 2007.

(46) Cosulich, S.; Griffen, E. New Thiazole Pyridine Sulfonamides as Orally Bioavailable Highly Potent PI3 Kinase Inhibitors. Presented at the 2007 Keystone Symposia, Santa Fe, NM, February 15−20, 2007.

(47) Adams, N. D.; Darcy, M. G.; Johnson, N. W.; Kasparec, J.; Knight, S. D.; Newlander, K. A.; Peng, X.; Ridgers, L. H. Preparation of *N*-Pyridinyl Benzenesulfonamide Derivatives as PI3 Kinase Inhibitors. PCT Int. Appl. WO2009055418A1, 2009.

(48) The suboptimal hydrogen bond angles between the Lys833 amino group and the sulfonamide oxygen (129°) and nitrogen (146°) atoms are the most likely explanation for this hydrogen bond not being observed.

(49) Fabian, M. A.; Biggs, W. H.; Treiber, D. K.; Atteridge, C. E.; Azimioara, M. D.; Benedetti, M. G.; Carter, T. A.; Ciceri, P.; Edeen, P. T.; Floyd, M.; Ford, J. M.; Galvin, M.; Gerlach, J. L.; Grotzfeld, R. M.; Herrgard, S.; Insko, D. E.; Insko, M. A.; Lai, A. G.; Lelias, J. M.; Mehta, S. A.; Milanov, Z. V.; Velasco, A. M.; Wodicka, L. M.; Patel, H. K.; Zarrinkar, P. P.; Lockhart, D. J. A Small Molecule−Kinase Interaction Map for Clinical Kinase Inhibitors. *Nat. Biotechnol.* **2005**, *23* (3), 329–336.

(50) A table of the studied kinases is presented in the Supporting Information.

(51) Compound **82** exhibited a bioavailability of 103% when administered as a 1 mg/kg dose in 20% Captisol, 2% HPMC, and 1% Tween 80, with the compound being dissolved at a pH of 9.0, and then the pH was readjusted to 7.

(52) Compound **73** was also evaluated in a a mouse liver (PD) assay, using dosages ranging from 0.01 to 0.3 mg/kg. Human HGF was injected iv 4 h postdose. The dose-response graph is included in the Supporting Information.

(53) Ali, I. U.; Schriml, L. M.; Dean, M. Mutational Spectra of PTEN/MMAC1 Gene: A Tumor Suppressor with Lipid Phosphatase Activity. *J. Natl. Cancer Inst.* **1999**, *91*, 1922–1932.

(54) Eng, C. PTEN: One Gene, Many Syndromes. *Hum. Mutat.* **2003**, *22*, 183–198.

(55) Rodenhuis, S.; van de Wetering, M. L.; Mooi, W. J.; Evers, S. G.; Van Zandwijk, N.; Bos, J. L. Mutational Activation of the K-ras Oncogene: A Possible Pathogenetic Factor in Adenocarcinoma of the Lung. *N. Engl. J. Med.* **1987**, *317*, 929–935.

(56) Okudela, K.; Hayashi, H.; Ito, T.; Yazawa, T.; Suzuki, T.; Nakane, Y.; Sato, H.; Ishi, H.; KeQin, X.; Masuda, A.; Takahashi, T.; Kitamura, H. *K-ras* Gene Mutation Enhances Motility of Immortalized Airway Cells and Lung Adenocarcinoma Cells via Akt Activation. *Am. J. Pathol.* **2004**, *164* (1), 91–100.

(57) Velho, S.; Oliveira, C.; Ferreira, A.; Ferreira, A. C.; Suriano, G.; Schwartz, J.; Duval, A.; Carneiro, F.; Machado, J. C. The Prevalence of PIK3CA Mutations in Gastric and Colon Cancer. *Eur. J. Cancer* **2005**, *41*, 1649–1654.

(58) Still, W. C.; Kahn, M.; Mitra, A. Rapid Chromatographic Technique for Preparative Separations with Moderate Resolution. *J. Org. Chem.* **1978**, *43* (14), 2923–2925.

(59) Gray, A.; Olsson, H.; Batty, I. H.; Priganica, C.; Downes, P. Nonradioactive Methods for the Assay of Phosphoinositide 3-Kinases and Phosphoinositide Phosphatases and Selective Detection of Signaling Lipids in Cell and Tissue Extracts. *Anal. Biochem.* **2003**, *313* (2), 234–245.

(60) Walker, E. H.; Pacold, M. E.; Perisic, O.; Stephens, L.; Hawkins, P. T.; Wymann, M. P.; Williams, R. L. Structural Determinants of Phosphoinositide 3-Kinase Inhibition by Wortmannin, LY294002, Quercetin, Myricetin, and Staurosporine. *Mol. Cell* **2000**, *6*, 909–919.

(61) Otwinowski, Z.; Minor, W. Processing of X-ray Diffraction Data Collected in Oscillation Mode. *Methods Enzymol.* **1997**, *276*, 307–326.

(62) Navaza, J. AMoRe: An Automated Package for Molecular Replacement. *Acta Crystallogr., Sect. A: Found. Crystallogr.* **1994**, *50*, 157–163.

(63) Murshudov, G. N.; Vagin, A. A.; Dodson, E. J. Refinement of Macromolecular Structures by the Maximum-Likelihood Method. *Acta Crystallogr., Sect. D: Biol. Crystallogr.* **1997**, *53* (Part 3), 240–255.

(64) Emsley, P.; Cowtan, K. Coot: Model-Building Tools for Molecular Graphics. *Acta Crystallogr. Sect. D: Biol. Crystallogr.* **2004**, *12* (Part 1), 2126–2132.

■ NOTE ADDED AFTER ASAP PUBLICATION

After this paper was published online February 18, 2011, three authors were added to the author list (Derin D'Amico, Longbin Liu, and Kevin Yang). The revised version was published March 1, 2011.